BULK SYSTEM ADEQUACY ASSESSMENT INCORPORATING WIND AND SOLAR ENERGY

A Thesis Submitted to the College of

Graduate Studies and Research

In Partial Fulfillment of the Requirements

For the Degree of Master of Science

In the Department of Electrical and Computer Engineering

University of Saskatchewan

Saskatoon, SK

By

SABBIR IBN ARMAN

PERMISSION TO USE

In presenting this thesis in partial fulfillment of the requirements for a Postgraduate degree from the University of Saskatchewan, it is agreed that the Libraries of this University may make it freely available for inspection. I also agree that permission for copying of this thesis in any manner, in whole or in part, for scholarly purposes may be granted by the professors who supervised this thesis work or, in their absence, by the Head of the Department of Electrical and Computer Engineering or the Dean of the College of Graduate Studies and Research at the University of Saskatchewan. It is strictly forbidden to do any copying, publication, or use of this thesis, or parts thereof, for financial gain without the written permission of the author. Proper recognition shall be given to the author and to the University of Saskatchewan in any scholarly use which may be made of any material in this thesis.

Request for permission to copy or to make any other use of material in this thesis in whole or in part should be addressed to:

Head of the Department of Electrical and Computer Engineering

57 Campus Drive

University of Saskatchewan

Saskatoon, Saskatchewan, Canada

S7N 5A9

ABSTRACT

Renewable energy sources have received increasing attention in electric power systems around the world due to growing environmental concerns. Wind and solar are among the most promising alternatives to conventional energy generation. There has been a rapid growth of wind and solar energy integration in power systems in the last decade, and is expected to grow further in the years to come.

The main concern with wind and solar energy sources is the uncertainty and the intermittency of power generation, which leads to problems in maintaining the overall system reliability. The impacts of these sources on bulk system reliability depend on a large number of factors. The strength of the wind or solar resource at the installation site, the existing renewable power penetration level in the system, the points of connection of these sources to the power grid, the correlation in resource availability between multiple installation sites, and the correlation between the load and the renewable power are key factors that are analyzed in this thesis. These factors are considered in evaluating the bulk system reliability and reliability benefits of wind and solar power sources, and the reliability worth to the electricity customers from the addition of these energy sources. The IEEE-RTS test system is utilized throughout the thesis to evaluate the effects of these factors on bulk system adequacy. Swift Current and Saskatoon wind resources are modeled and utilized in this thesis. The Swift Current area has a strong wind resource and provides better reliability benefit and reliability worth than the Saskatoon wind resource. The benefits from wind and solar power integration, however, also depend significantly on the location where it is connected to the grid network. Wind farms that are diversified in multiple regions with independent wind speed profiles provide superior reliability benefits and worth than wind farms located in one region. The incremental benefits of adding wind or solar power decreases as the

renewable power penetration is increased in the power system. Wind power at practical locations provides higher reliability benefits than photovoltaics. However, the daytime contribution of photovoltaics to system reliability is relatively high. The reliability benefits and reliability worth of solar power are significantly different for different seasons. A comparison study on reliability benefit and worth between a wind integrated bulk system and a solar integrated bulk system is also done in this thesis in order to identify the best option for bulk system reliability.

ACKNOWLEDGMENTS

I would like to express my deepest gratitude and sincere appreciation to my supervisors Dr. Rajesh Karki and Dr. Roy Billinton for their persistent veteran guidance, support as well as constant patience, motivation, financial support and immense knowledge throughout my research and writing this thesis. It is very difficult to express my sincere gratitude within a few words because the more I express about them the more will be less.

I am also very much grateful to my graduate study teachers, Dr. Sherif O. Faried and Dr. Ramakrishna Gokaraju for outstanding support on strengthening my perception on power system analysis and power system protection. I would also like to thank the College of Graduate Studies and Research, and the Department of Electrical and Computer Engineering for providing support throughout my graduate program. My earnest thanks to my committee members for their valuable comments, suggestions and inputs in my thesis improvement. I am very much thankful to all my colleagues in the Power System Research Group in University of Saskatchewan for their support during my M.Sc. program.

Last but surely not the least, I am truly grateful to my parents, Md. Armanuzzaman and Shahida Akhter, my brother Tanvir Arman and my fiancée Hossain Stefania for their constant support, motivation, encouragement and love throughout my M.Sc. thesis.

TABLE OF CONTENTS

LIST OF TABLES

LIST OF FIGURES

LIST OF ABBREVIATIONS

ARMA	Auto-Regressive and Moving Average
CanWEA	Canadian Wind Energy Association
CCS	Customers' Cost Savings
CEA	Canadian Electricity Association
COPT	Capacity Outage Probability Table
CSP	Concentrated Solar Power
EDC	Expected Damage Cost
EDLC	Expected Duration of Load Curtailment
EENS	Expected Energy Not Supplied
EPSRA	Electric power system Reliability Assessment
ERIS	Equipment Reliability Information System
ESRB	Expected Solar Reliability Benefit
EWRB	Expected Wind Reliability Benefit
FOR	Forced Outage Rate
GW	Gigawatt
HL	Hierarchical Level
HL-I	Hierarchical Level I
HL-II	Hierarchical Level II
HL-III	Hierarchical Level III
hrs	Hours
hrs/yr	Hours per Year
H_T	Hourly Solar Radiation

H_{Tr}	Solar Radiation in a Standard Environment
IEAR	Interrupted Energy Assessment Rate
IEC	International Electrotechnical Commission
IEEE	Institute of Electrical and Electronic Engineering
IPLCC	Increased Peak Load Carrying Capability
MECORE	Monte Carlo Evaluation of COmposite system Reliability
MRTS	Modified Reliability Test System
MW	Megawatt
MWh	Megawatt-hour
occ.	Occurrence
OPF	Optimal Power Flow
p.u.	Per Unit
PDR	Probability of Single Derated State
PLCC	Peak Load Carrying Capability
P_R	Rated Power Output
PV	Photovoltaics
PVCS	Photovoltaics Conversion System
RTS	Reliability Test System
WTG	Wind Turbine Generator
yr	Year

1 INTRODUCTION

1.1 Power System Reliability

Electric energy is essential to mankind in the modern world. Future development is highly dependent on reliable power supply being available to the customers at a reasonable price. Power system planners need proper assessment tools for planning adequate generation and transmission capacity in order to provide an uninterrupted power supply to the consumers and meet their electricity demand at all times. The likelihood of a continuous and reliable power supply can be assessed through reliability studies. Power system reliability analysis is required to examine the power system behaviour and assess the ability of the system to satisfy the system demand at an acceptable reliability level [1, 2].

Power system reliability assessment can be divided into the two areas of system adequacy and system security [1] as illustrated in Figure 1.1. System adequacy is focussed in the existence of sufficient facilities to meet the system's customer demand and provide uninterrupted power supply to all the customer loads through the system transmission and distribution network. System adequacy evaluation examines static system conditions rather than dynamic disturbances in the system. System security assessment, on the other hand, examines the ability to respond to disturbances that may arise during system operation, and is associated with dynamic conditions of the system [1]. System adequacy and security analyses are both important in ensuring that the system meets the load demand at all times, and minimizing customer costs due to power outages. This thesis is focussed on the adequacy analysis of power systems.

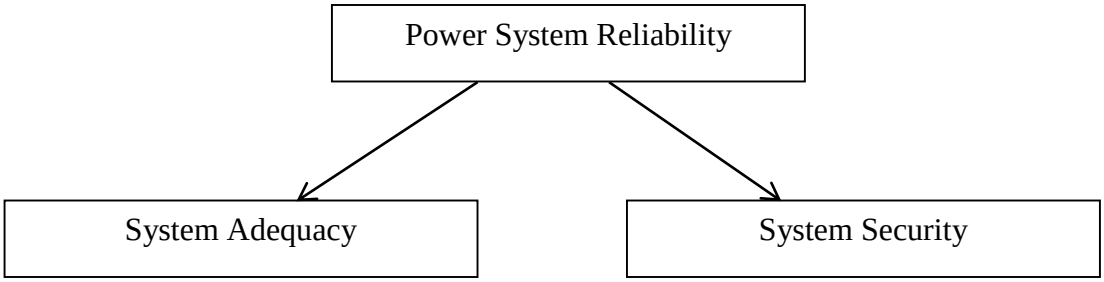

Figure 1.1: Subdivision of power system reliability

A modern electric power system is a huge interconnected complex entity. It is extremely difficult to carry out a reliability evaluation of the whole interconnected system. Reliability studies of power systems are therefore usually divided into three hierarchical levels (HL) [1] as shown in Figure 1.2 to conduct comprehensible reliability analysis. The three hierarchical levels are generation, transmission and distribution [1, 3, 4]. Hierarchical level I (HL-I) analysis refers to the ability of the generation capacity to meet the total system load without considering transmission and distribution facilities. Hierarchical level II (HL-II) studies, also designated as composite or bulk system analysis, are done considering both generation and transmission facilities to meet the total system demand. Hierarchical level III (HL-III) assessment considers all three generations, transmission and distribution facilities in the evaluation. HL-III analysis is usually done for past performance assessment; as predictive analysis is very complex at this level. Predictive reliability studies are often done at the distribution system level, and can be extended to HL-III using HL-II results as inputs. This thesis is focussed on bulk system (HL-II) adequacy evaluation considering both generation and transmission facilities.

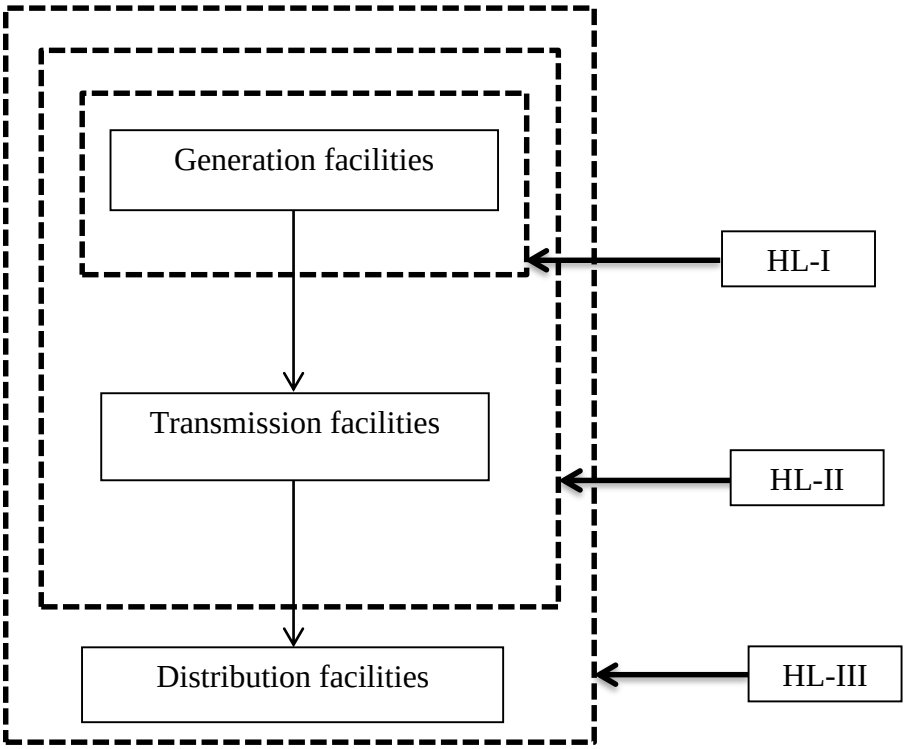

Figure 1.2: Hierarchical levels

1.2 Power Systems with Wind Energy

Renewable energy sources are slowly replacing conventional energy sources as they are considered to be clean and easily accessible electricity sources. Wind energy is more widely used than other renewable sources. Wind projects can be installed in less time than many other power generation plants, and the cost of wind energy technology is decreasing. In recent years massive investments have been made on wind energy in power systems globally. This has accelerated the advancement of wind power technologies. There is no fuel cost associated with wind energy production and therefore wind energy has an economic advantage over more conventional energy sources. The owner of a wind farm can estimate the cost of electricity production before wind farm establishment using wind regime data. It may be more difficult to forecast the electricity

production cost for conventional plant owners due to fuel price variability. Fuel prices fluctuate based on demand, foreign exchange, geographic location, local competition and many other factors. Canada's total installed wind capacity (at the end of year 2015) is over 11,000 MW. In the year 2015 alone, Canada installed 1506 MW of wind power from 36 wind energy projects [5]. The current installed wind capacity supplies around 5% of Canada's electricity demand [5]. This is equivalent to meeting the needs of over 3 million homes in Canada [5]. The province of Saskatchewan has 221.3 MW of wind capacity located in the southern part of the province as shown in Table 1.1.

Table 1.1: Saskatchewan wind farms and their installed capacity (Dec 31, 2015) [5]

Project Name	**Year**	**Total Capacity (MW)**
Cypress Wind Power Facility	2001 & 2003	10.5
Sunbridge	2001	11.2
Centennial Wind Power Facility	2006	149.4
RedLily Wind Energy Project	2011	26.4
Cowessess First Nation Wind and Storage Demonstration Project	2013	0.8
Morse Wind Project	2015	23

Wind energy projects are increasing around the world. Global wind power capacity was 432.48 Gigawatts (GW) in 2015 [6]. This is a 17% increase on the 2014 global wind power capacity [6]. Figure 1.3 shows the global cumulative wind power capacity from the year 2000 to 2015. Wind capacity increased rapidly from 6.1 GW in 1996 to 369.69 GW in 2014 [6]. As shown in Figure 1.3, wind power has been growing rapidly in the last few years, and the market research indicates that considerably more wind power will be installed in the next decade.

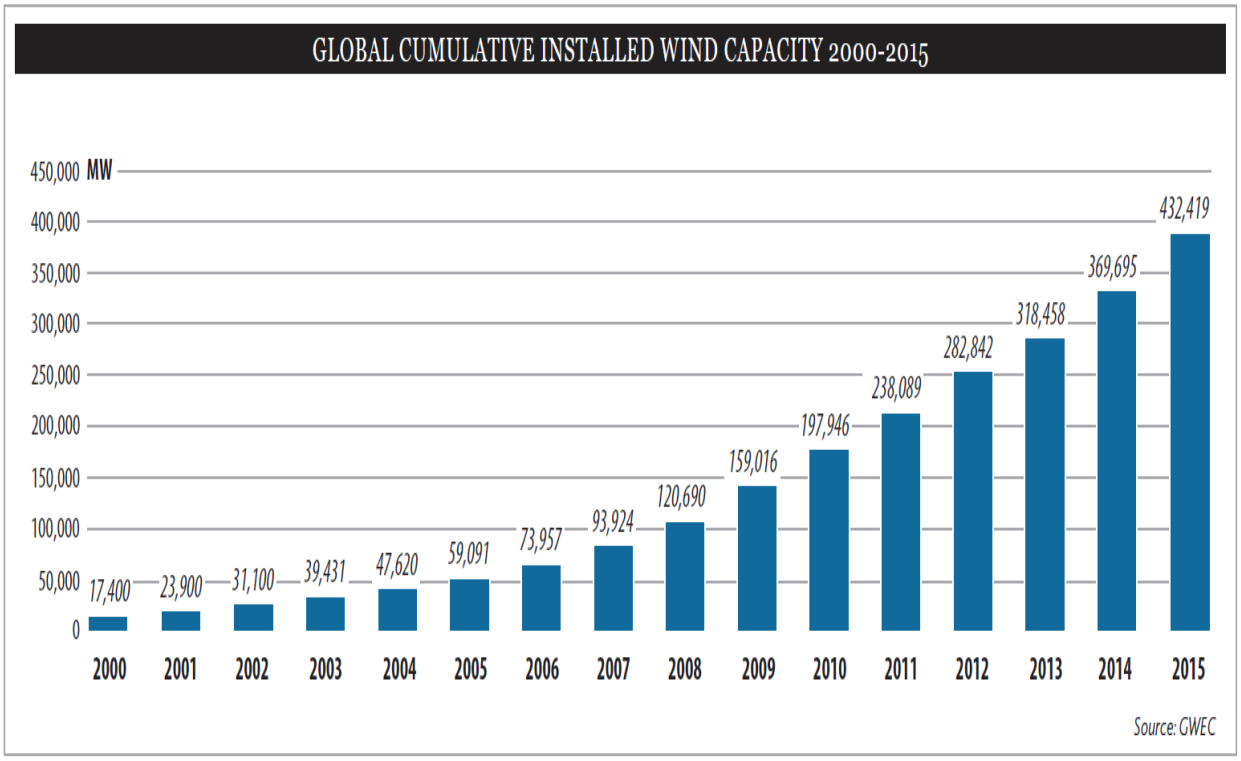

Figure 1.3: Cumulative world wind installed capacity (source: global wind energy council, www.gwec.net)

Wind energy is highly variable and site specific, and its characteristics are therefore, very different from those of the conventional energy sources. Wind power output is uncertain, and can vary from zero to the rated capacity value depending on the wind speed at the wind power site. Evaluation models to represent wind energy sources are different from the models used for conventional energy sources. The wind turbine generator (WTG) is the key component in the conversion of wind energy into electricity. The WTG characteristics and the wind speed regime at the wind site are important parameters in adequacy evaluation.

1.3 Power Systems with Solar Energy

Solar power is recognized as an alternate renewable energy source that has high potential for large scale application in electric power generation. Electricity is produced from sunlight in mainly two ways; photovoltaics (PV), and concentrated solar power (CSP) [7]. In the PV

technology, sunlight is directly converted into electrical energy by photovoltaic cells. The CSP technology primarily uses mirrors to concentrate the solar irradiation to generate steam for electricity production. The work reported in this thesis is focused on PV technology, which requires relatively less maintenance, and generates electricity that is free of carbon emissions. Many developed countries are increasingly using solar energy as an alternate source to offset burning fossil fuels and reduce carbon emissions. The use of PV is also growing in the developing countries since this resource is available almost everywhere and is cost effective in rural communities that are far away from the power grid.

The installed capacity of PV in Canada increased sharply after the year 2009 in four submarkets; the stand-alone domestic, standalone non domestic, grid connected distributed, and grid connected centralized [8]. The total cumulative PV installed capacity in the year 2009 was 94.57 MW, which grew to over 1800 MW in year 2014 as shown in Figure 1.4. Global PV solar capacity increased in the last decade as shown in Figure 1.5. The global installed PV capacity in year 2014was 177 Gigawatts (GW) and increased from 3.7 GW in year 2004 [9]. Compared to 2012, the installed PV capacity increased by 39% in 2013 [9]. The growth in global PV capacity is expected to continue in the next decade.

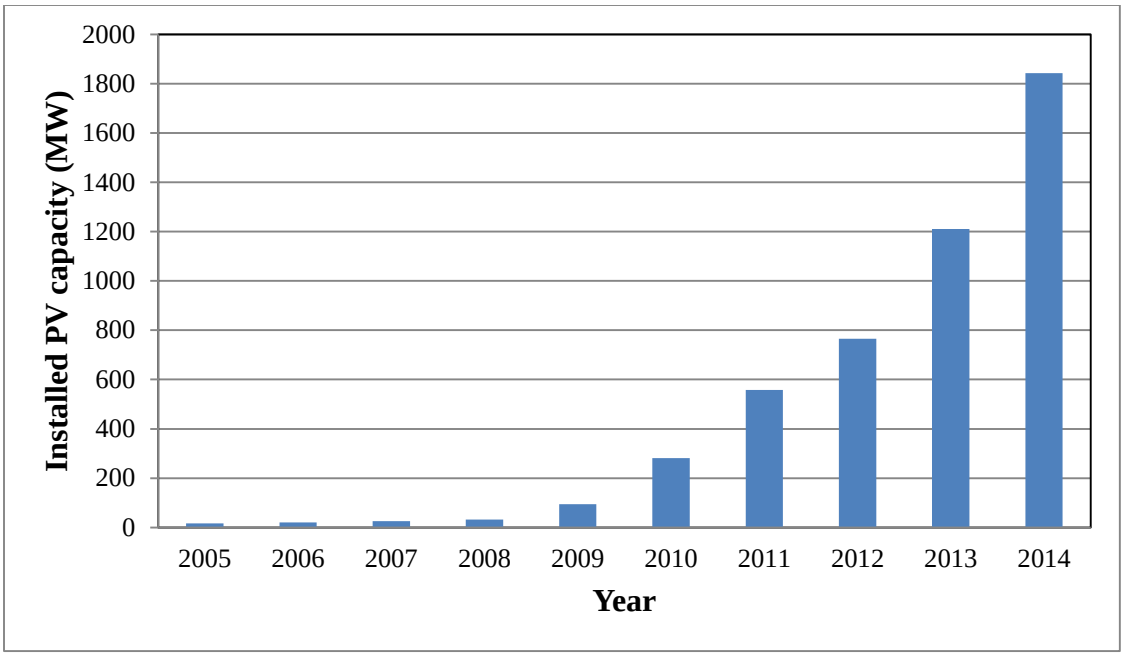

Figure 1.4: Cumulative installed PV capacity in Canada (source: national survey report of PV power applications in Canada 2014)

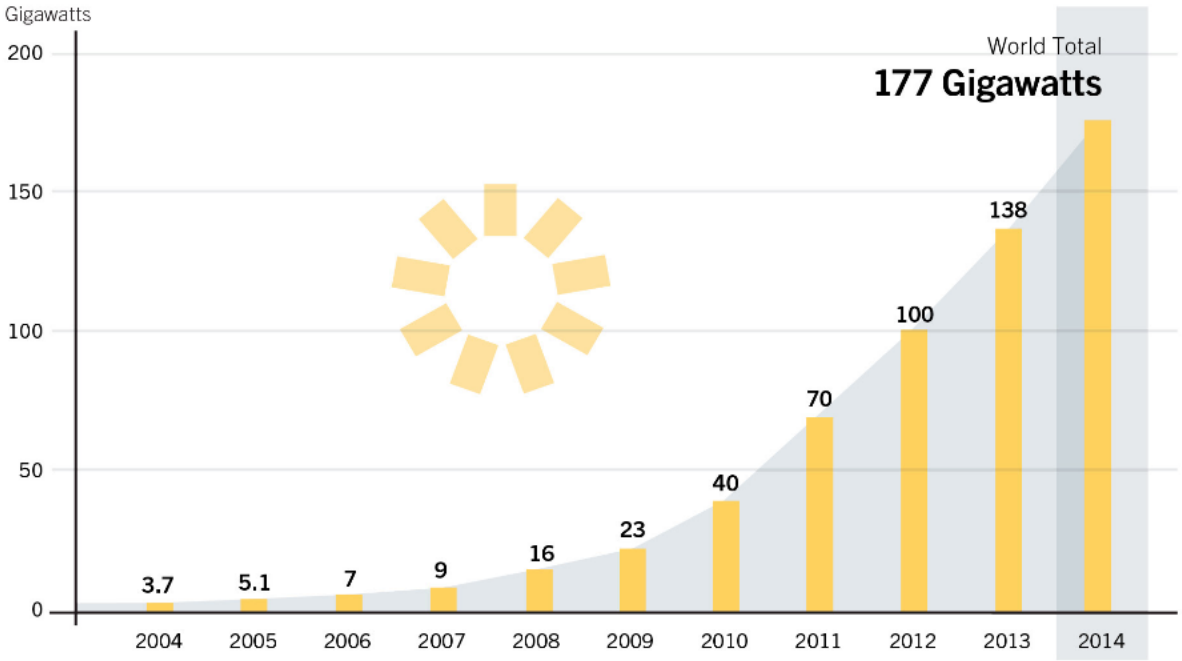

Figure 1.5: Total global solar PV capacity, 2004-2014 (source: REN21, 2015, renewables 2015 global status report)

Solar power is unavailable at night and variable during the day depending on the solar radiation at the specific site. The variation in available power from PV sources creates challenges to system planners in planning adequate generation and transmission facilities to effectively meet the load demand. PV technology has advanced with improved cell technology, inverter technology, maximum power point tracking, and solar tracking systems. Adequacy evaluation of power systems using solar energy have been studied at the HL-I level by several researchers [31-34]. Limited studies are reported on system adequacy using solar energy at the HL-II level. This thesis is focused on adequacy evaluation of the PV integrated power system at the HL-II level.

1.4 Problem Statement and Research Objectives

Wind and solar energy are considered to be the most important renewable energy sources in power systems. The power output of both wind and PV sources are highly variable in nature which adds considerable difficulty in planning generation and transmission systems in order to meet the system load at acceptable risk levels. A large number of research activities have been reported in reliability analysis of power systems with conventional generating units, and a wide range of techniques [10-15] have been developed and used in capacity planning. These methods have been modified over time to include wind energy. Literature on the reliability studies of power systems incorporating wind resources have been published utilizing both simulation and analytical techniques [16-25]. There has been similar research work done on reliability studies of power systems containing PV sources. A number of different methods to model the variability in power production from PV sources are available [26-28] and reliability studies of power systems incorporating PV have been conducted using both analytical and simulation methods [29, 30, 10, 12]. References [31-33] present adequacy benefits of power systems integrated with solar energy. The impact of adding PV in a power system is assessed to observe the reliability contribution of

PV at the HL-I level in [34]. There is limited work on bulk system reliability incorporating solar and wind energy.

HL-II studies are commonly referred to as composite or bulk system studies in power system reliability evaluation. Bulk system adequacy evaluation considers the ability of both the generation and transmission facilities to satisfy the demand and energy supplied to the bulk system load points based on the load curtailment philosophy in the power system [11]. Bulk system adequacy analysis can be done using analytical procedures, Monte Carlo simulation techniques, or a combination of these two methods [10-12]. Analytical methods do not readily integrate the chronological characteristics of solar irradiation or wind speed to assess the reliability of these energy resources in power systems [35]. In this thesis, bulk system adequacy analysis is carried out using the Monte Carlo simulation method in the MECORE software [1, 29]. A number of papers [10-12] has been published on mathematical modeling of solar or wind for reliability evaluation of power systems. Both analytical and Monte Carlo simulation methods have been used to assess composite system adequacy considering wind and solar energy sources in [19]. This work presents adequacy analysis of a composite power system considering single and multiple independent wind or solar energy facilities. The reliability impact of adding wind and solar power at different bus locations of a power system was investigated in [19]. Reference [36] investigated the load forecast uncertainty and the wind speed correlation factor in bulk system adequacy but did not consider solar power. The reliability contribution of added wind or solar power depends significantly on the grid connection point in the power system due to the inherent reliability designed into the network topology. It is equally important to consider the strength of the renewable resource available at the different network locations where these resources can be injected into the power system. A composite generation and transmission system reliability study

can be used to identify optimal network bus locations to inject new generation to provide maximum reliability benefits to the system. The wind regime at an optimal bus location may, however, be relatively poor. On the other hand, the transmission network at a strong wind regime may be insufficient, and additional transmission may be required to exploit the generated wind power. Renewable energy growth usually involves installing wind turbines in more remote areas and/or adding wind turbines to those operating in areas with good wind regimes, which will eventually result in congestion of the transmission lines and reduction in the reliability benefits to the bulk system. A comprehensive analysis of these factors and their impacts on the bulk system reliability is, therefore, necessary to resolve these concerns in decision making during wind energy planning.

A major drawback of significantly expanding wind capacity at a single location with a strong wind regime is that the power outputs of all the wind turbine generators are dependent on the same wind regime. Past research [36] on wind integrated bulk system adequacy analysis considering wind speed correlation show that the reliability contribution of renewable energy sources can be significantly improved by distributing the resources at multiple sites with diverse resource characteristics. The studies show that the reliability benefits increase as the degree of wind speed correlation between two wind farm sites decreases. Diversifying wind resources normally causes selecting wind farm locations with wind regimes that are poorer than the present wind farm regimes, or building wind farms in the remote areas that will involve relatively high transmission upgrades. Comprehensive composite system reliability assessment is therefore very important in decision making in regard to new wind and PV site selection.

The work in this thesis is focused on bulk system adequacy evaluation. The main objectives of this thesis are to develop methodologies to quantify the reliability benefits from the integration of wind and solar power in electric power systems considering the impacts of integration point in

the grid network, strength of the renewable resource at the connection point, resource penetration level, resource characteristics and diversification, and comparison between the benefits from wind and solar integration in the bulk system adequacy. The first step in bulk system adequacy evaluation considering wind and PV is to develop appropriate wind and solar power model using hourly wind speed and hourly solar radiation data. These models need to be integrated in the MECORE software for bulk system reliability evaluation. A range of studies with different wind regimes and penetration levels can be carried out to analyze the impact on bulk system reliability of resource strength and characteristics. Reliability studies considering wind power integration at different network locations in the bulk system can be done to obtain a better understanding of the comparative impact between the resource strength and the connection point, and can lead to the development of better strategies in wind farm establishment planning. Another important factor is the diversification of wind resources by distributing wind farm installations at different network locations. Diversifying wind power capacity to different locations in the network can provide increased reliability benefits, which can be quantified.

The impact of PV penetration in a bulk system is another important topic to investigate as PV installations continue to increase in power systems around the world. As solar power is only available during the daytime, it is important to assess how daytime PV contribution impacts bulk system reliability. It is also important for power system planners to assess the reliability worth of adding wind and solar energy sources in renewable energy planning and investment. Results from reliability worth analysis provide important information on the actual cost savings and energy reliability benefit of renewable sources. The objectives of the research work reported in this thesis are summarized in the following steps:

1. The development of appropriate wind and PV models for bulk system adequacy evaluation using the Monte Carlo simulation method programmed in the MECORE software.
2. Examination of the adequacy impacts of the wind resource strength in a bulk power system.
3. Study of the relative impact of wind regime strength and network injection point on bulk power system adequacy.
4. Investigation of the impact of wind farm diversification in different sites of power systems.
5. Study of the bulk system reliability impact of PV penetrations, the daytime solar contribution and seasonal contributions to the bulk power system adequacy.
6. Analysis of the reliability worth of renewable energy sources and comparing the reliability and cost implications of wind and PV in power systems.

1.5 Thesis Outlines

This thesis consists of six chapters. The main content of each chapter is described below.

Chapter 1 provides background information on reliability concepts in electric power systems, and describes reliability assessment at different functional zones or hierarchical levels. Wind and solar are the most widely used renewable energies in the world, and statistics on their rapid growth in Canada and around the world are presented. The importance of bulk system reliability evaluation including renewable energies such as wind and solar is briefly discussed considering the global increase in installed capacity of wind and solar energy sources. Reliability assessment of electric systems integrated with renewable energy sources is briefly discussed. The main objectives of the research are outlined.

Chapter 2 discusses the basic and IEEE proposed reliability indices for bulk system adequacy analysis. This chapter describes the concepts of Monte Carlo simulation, and the different types of simulation techniques. The MECORE commercial software is introduced in this

chapter where state sampling Monte Carlo simulation is utilized to obtain the bulk system reliability indices. This chapter also presents base case studies of the IEEE Reliability Test System (RTS) using the MECORE software.

Chapter 3 presents the development of the wind power model and photovoltaic power model integrated with MECORE. Wind speed data obtained from Environment Canada was utilized to develop the wind power model for Swift Current and Saskatoon wind sites. Solar radiation data for the Swift Current area were simulated using the SIPSREL+ software, and was used to obtain the PV power model. Daytime and seasonal PV models were also developed. These models can be integrated in the MECORE software for bulk system adequacy evaluation.

The developed wind power models are used to conduct a range of adequacy assessment of a wind integrated power system in Chapter 4. Different case studies are presented to illustrate the impact of wind regime strength, grid network connection point, wind energy growth and wind farm diversification. The impact of transmission line outages is also analyzed in this chapter. The reliability and cost contribution of wind energy considering the above described factors are summarized at the end of this chapter.

Chapter 5 presents PV integrated bulk system adequacy analysis based on solar installed capacity, daytime solar and seasonal contributions. Solar energy reliability benefit and customer outage cost saving are also analyzed and presented in this chapter. At the end of this chapter, PV and wind energy sources are compared in terms of their adequacy benefits and reliability benefits to the system.

Chapter 6 presents the conclusions and a summary of the thesis.

2 BULK POWER SYSTEM ADEQUACY ASSESSMENT

2.1 Introduction

The main function of a bulk power system is to generate and provide electricity to the major load points and assure the continuity of adequate electricity at these load points. Bulk system adequacy evaluation is complex because both generation and transmission contingencies are involved with this evaluation [29]. Bulk system reliability analysis requires load flow studies, generation rescheduling and contingency assessment to analyze if the system can maintain adequate voltage levels, meet the system load at various conditions, and provide acceptable system behaviour during contingency situations. Load curtailment philosophies and transmission overload alleviation methods are also important in bulk system analyses due to generation deficiencies and line load allocation adjustments. Power system planners have to determine the acceptable level of power generation to satisfy the load requirement taking into account factors such as unpredictable system loads, load curtailment philosophies, forced outage rates of the generating units and the intermittent generation sources [10]. A reliable transmission network to carry energy from the generating points to the load points is an important factor in the bulk system adequacy evaluation [37]. Probabilistic load flow considering both the generation and transmission facilities are illustrated in [10]. Research on bulk system reliability assessment using sequential Monte Carlo simulation is presented in [11].

Both analytical and Monte Carlo techniques have been used for bulk system adequacy assessment. In an analytical technique, the system is represented by analytical models and mathematical solutions are utilized to compute the system adequacy indices from these models. Monte Carlo simulation mimics the random behaviour of the system to assess the adequacy indices

[36]. Both these methods have their merits and demerits, and have been used in bulk system adequacy evaluation. The work reported in this thesis utilizes Monte Carlo simulation and the approach used is described later in this chapter.

2.2 Reliability Indices for Bulk System Analysis

Reliability indices provide a quantitative assessment of the bulk system adequacy. There are two types of reliability indices, the load point indices and the system indices. The load point indices describe the individual load point adequacy, whereas, the system indices provide a quantitative assessment of the total system [38]. Load point indices and system indices have different uses, and are obviously related to each other. The system indices are important in comparing the overall system performance when considering alternate planning or system upgrade schemes. Load point indices can be used to identify individual weak buses in the system that require improvement. Bulk system reliability indices can be created and categorized as predictive indices and past performance indices [40]. Past performance indices are calculated from data collected from the actual operation of the bulk system, and provide a quantitative assessment of system behaviour. Predictive indices provide useful information on the risks associated with the future behaviour at the load points and the overall system. These indices are dependent on the reliability performance of both the generation and transmission facilities [40]. The Canadian Electricity Association (CEA) collects and disseminates component outage data and system past performance data respectively through their Equipment Reliability Information System (ERIS) and the Electric Power System Reliability Assessment (EPSRA) for power utilities in Canada [40]. Bulk system adequacy assessment can be done using a wide range of adequacy indices. The basic load point reliability indices and IEEE proposed [29, 39] system indices are defined as follows.

(a) Basic Indices

(1) Probability of Load Curtailment (PLC)

$$\text{PLC} = \sum_{i \epsilon S} P_i \tag{2.1}$$

Where P_i is the probability of system state i and S is the set of all system states associated with load curtailments.

(2) Expected Number of Load Curtailment (ENLC)

$$\text{ENLC} = \sum_{i \epsilon S} F_i \ \ occ./yr \tag{2.2}$$

The ENLC is the sum of the occurrences of the load curtailment states and is therefore an upper boundary of the actual frequency index. The system state frequency F_i can be calculated by the following relationship between the frequency and the system state probability P_i.

$$F_i = P_i \sum_{K \epsilon N} \lambda_K \ \ occ./yr \tag{2.3}$$

Where λ_k is the departure rate of component k and N is the set of all components of the system.

(3) Expected Duration of Load Curtailment (EDLC)

$$\text{EDLC} = \text{PLC} \times 8760 \text{ hrs/yr} \tag{2.4}$$

(4) Average Duration of Load Curtailment (ADLC)

$$\text{ADLC} = \text{EDLC/EFLC hrs/disturbance} \tag{2.5}$$

(5) Expected Load Curtailment (ELC)

$$\text{ELC} = \sum_{i \epsilon S} C_i \ F_i \text{MW/yr} \tag{2.6}$$

Where C_i is the load curtailment of system state *i*.

(6) Expected Demand Not Supplied (EDNS)

$$\text{EDNS} = \sum_{i \epsilon S} C_i \ P_i \text{MW} \tag{2.7}$$

(7) Expected Energy Not Supplied (EENS)

$$\text{EENS} = \sum_{i \epsilon S} C_i F_i D_i = \sum_{i \epsilon S} 8760 C_i P_i \text{ MWh/yr} \quad (2.8)$$

Where D_i is the duration of system state *i*.

(8) Expected Damage Cost (EDC)

$$\text{EDC} = \sum_{i \epsilon S} C_i F_i D_i W \text{ k\$/yr} \quad (2.9)$$

Where C_i is the load curtailment of system state i; F_i and D_i are the frequency and the duration of system state i; W is the unit damage cost in \$/kWh.

(b). IEEE Proposed Indices

(9) Bulk Power Interruption Index (BPII)

$$\text{BPII} = \frac{\sum_{i \epsilon S} C_i F_i}{\sum_{i \epsilon S} L_i} \text{ MW/MW-yr} \quad (2.10)$$

Where L is the annual system peak load in MW

(10) Bulk Power/Energy Curtailment Index (BPECI)

$$\text{BPECI} = \frac{EENS}{L} \text{ MWh/MW-yr} \quad (2.11)$$

(11) Bulk Power-supply Average MW Curtailment Index (BPACI)

$$\text{BPACI} = \frac{ELC}{EFLC} \text{ MW/disturbance} \quad (2.12)$$

Where EFLC is the expected frequency of load curtailment:

$$\text{EFLC} = \sum_{i \epsilon S} (F_i - f_i) \text{ occ./yr} \quad (2.13)$$

F_i is the frequency of departing system state i and f_i is the portion of F_i which corresponds to not going through the boundary wall between the loss-of-load state set and the no-loss-of-load state set.

(12) Modified Bulk Energy Curtailment Index (MBECI)

$$\text{MBECI} = \frac{EDNS}{L} \text{MW/MW} \tag{2.14}$$

(13) Severity Index (SI)

$$\text{SI} = \text{BPECI} \times 60 \text{ system min/yr} \tag{2.15}$$

(14) Delivery Point Unreliability Index (DPUI)

$$\text{DPUI} = \frac{\text{Total Unsupplied Energy}}{\text{System Peak Load}} \text{ MW-Minutes/MW} \tag{2.16}$$

The advantage of normalized indices is that they can be used for comparison of the system adequacy of different sized systems. They are analyzed for the overall system. Basic indices are applied for individual load point or overall system analysis. These indices can be evaluated at a particular system peak load (annualized indices) or based on the system load duration curve (annual indices).

2.3 Monte Carlo Simulation

Monte Carlo simulation is a process involving repeated samples or trials of system scenarios obtained using random numbers in a probabilistic technique. This method is more flexible than analytical methods when complex actual system situations need to be recognized in the evaluation. A remarkable amount of research has been done in power system reliability evaluation using Monte Carlo simulation [11], and the different Monte Carlo techniques are compared in [39]. The major advantages of MCS over an analytical method are as follows.

1. MCS can provide the probability distributions of the adequacy indices, which cannot be easily obtained with analytical methods.

2. MCS can maintain chronology of events, and therefore model the dependent characteristics of reservoir operating conditions in hydro systems, weather effects, correlation between events, etc.
3. In large scale systems MCS can provide acceptable high level accuracy by using large number of trials of system scenarios.

Sequential simulation and non-sequential simulation are the two general Monte Carlo simulation methods [46]. Sequential simulation recognizes the chronological behaviour of component states and system events [46]. The non-sequential method is a more widely used method for power system reliability analysis as the sequential method requires considerable computation time to generate and store information on the entire system components' chronological state transition processes in a long time length [46]. The non-sequential method can be divided into state sampling and state transition sampling [44] types. A non-sequential state sampling approach is described below.

2.3.1 Non-Sequential State Sampling Approach

In the state sampling approach, a system state can be determined by considering combinations of all the component states. Each component state can be found by sampling using the reliability data for that component [41-43]. The chronological event behaviour is ignored in this approach. The sampling of the component state is established by generating random numbers. Each component characteristic is represented by a uniform distribution between [0, 1]. A component can reside in one of two or more states depending on it's behaviour. In a two-state component model, the two states are denoted as failure and success, where component failures are independent events. The state of a system consisting of r components can be denoted by the vector $S = (S_1, S_2, S_3, \ldots\ldots S_i, \ldots.. S_r)$. The vector S consists of r components including generators,

transmission lines, transformers, etc. [39]. S_i represents the state of the ith component. If S equals zero then the system is in the normal state. If S is other than zero, the system is in a contingency state because of component outage. The process of this method is summarized in the following steps.

1. A uniform random number U_i is generated for the i_{th} component.
2. The state of the component *i* can be determined using the following expression:

$$S_i = \begin{cases} 0 \quad (success\ state) & if Ui \geq FORi \\ 1 \quad (failure\ state) & if\ 0 \leq Ui < FORi \end{cases} \tag{2.17}$$

   Here, FOR*i* is the forced outage rate of the i_{th} component

   Multi-state components with their derated state probabilities can be considered in the simulation process without any major increase in the required calculation time [50]. The probability of a single derated state for the i_{th} component is denoted as PDR_i and the probabilities of the i_{th} component including a single derated state for step 2 can be expressed using the following equation.

$$S_i = \begin{cases} 0 \quad (Up\ State) & if\ Ui \geq PDRi + FORi \\ 1 \quad (Down\ State) & if\ PDRi \leq Ui < PDRi + FORi \\ 2 \quad (Derated\ State) & if\ 0 \leq Ui < PDRi \end{cases} \tag{2.18}$$

3. The system state S can be determined by implementing step (2) for all components.
4. Decide the system state. If S series has any non-zero values then the system is in a contingency state but S equals zero implies the normal state of the system.
5. If the system state results in a load curtailment, a linear programming optimization model is utilized to reschedule generation, lessen line overloads and to elude load curtailment if possible or to lessen the total load curtailment if inevitable [42].

6. The adequacy indices for each load point and overall system are collected and step (1) to (5) repeated until the stopping criterion is achieved.

2.4 Introduction to the MECORE Software

MECORE stands for Monte Carlo Evaluation of COmposite system Reliability (MECORE). This software was first developed at the University of Saskatchewan and later enhanced by BC Hydro [38]. MECORE is a Monte Carlo based simulation tool designed for reliability and reliability worth analysis of composite generation and transmission systems. It can also be used for adequacy evaluation of a bulk or composite generation and transmission system. It can provide a set of load point indices as well as overall system indices. Load point indices are highly dependent on load curtailment philosophy. Individual load point indices are accumulated to obtain a set of system indices that represent overall evaluation of the whole system. MECORE uses state sampling Monte Carlo simulation and enumeration techniques to analyze the power system. System component states are simulated using the state sampling method, and the annualized indices are calculated at the system peak load level. An enumeration technique is used to calculate annual indices using the annual load curve [38]. Multi-state random variables are used to model generating unit states. MECORE was initially designed to incorporate only two state models to represent generating units. It was later modified to incorporate up to ten derated states in order to represent multi-state renewable energy generation units, such as wind turbine units. Two state models are used to represent each transmission line in the system. MECORE uses a DC load flow and a linear programming optimal power flow (OPF) model for generation rescheduling, alleviating line overloads in order to avoid load curtailments if possible or reduce total load curtailment if it is inevitable.

MECORE uses priority order to make load shedding decisions to lessen system constraints. Priority order is done based on economic factors that distinguish the customer cost associated with failure or supply. Interrupted Energy Assessment Rate (IEAR) is an important index to account for the customer outage loss as a function of energy not supplied [1]. A higher value of IEAR indicates a more disruptive loss of supply, which has a higher priority order. The IEAR for the overall system is calculated using following equation [1].

$$\text{system IEAR} = \sum_{k=1}^{NB} IEAR_k q_k \quad (2.19)$$

Where NB is the total number of load buses in the system, $IEAR_k$ is the IEAR at load Bus k, and q_k is the fraction of the system load utilized by the customers at load Bus k.

The capabilities of the MECORE software are summarized below [38].

a) System Size

- MECORE is designed to handle up to 1000 Buses and 2000 Branches

b) System Analysis

- Generation Outages only: The failure data of transmission lines/ transformers are ignored
- Transmission Outages only: Generating units failure data is ignored
- Both Generation and Transmission Outages: The failure data of both generating and transmission facilities are taken into account.

c) **Failure modes**

- Independent failures of generators, lines and transformers
- Common cause outages of transmission lines
- Generating unit derating states

d) **Failure criteria**

- Capacity deficiency
- Line overload
- System separation-load loss
- Bus isolation-load loss

e) **Load model**

- Annual, seasonal, and monthly load curve
- Multi-step models
- Bus load proportional scaling and flat level model

f) **Probability indices**

- System indices and load point indices
- Annualized and monthly/seasonal/annual indices
- Basic and IEEE-proposed indices

  The basic indices include the ENLC, ADLC, EDLC, PLC, EDNS, EENS, EDC and ELC. The IEEE-proposed indices include the BPII, BPECI, BPACI, MBECI, and SI. The ENLC, ADLC, EDLC, PLC, EDNS, EENS, EDC, BPII, BPECI, BPACI, MBECI and SI are calculated at the system level, The ENLC, PLC, ELC, EDNS and EENS are calculated for each individual load point.

2.5 The Composite Test System

An educational test system known as the IEEE Reliability Test System (IEEE-RTS) [47] was used to conduct the research work in this thesis. A single line diagram of the IEEE-RTS is shown in Figure 2.1. The IEEE Task Force developed the IEEE-RTS as a common test system for

research and comparative studies. The IEEE-RTS generating system consists of 32 generators whose capacities vary from 12 MW to 400 MW. The transmission system has 24 Buses including 10 generator Buses, 10 load Buses and 4 common Buses. They are connected by 33 transmission lines and 5 auto transformers at two voltage levels which are 138 kV and 230 kV. The IEEE-RTS has 3405 MW of total installed capacity and the system peak load is 2850 MW. The IEEE-RTS uses the per unit load model designated as the IEEE-RTS load model [1, 29]. Chronological loads of 8760 hours on a per unit basis can be obtained from the IEEE-RTS load model. The basic data for this test system is provided in the Appendix.

2.6 Base Case Studies for the IEEE-RTS

Base case studies for any system are important to create a reference structure for better understanding of system modification and data sensitivity analysis. Various factors such as multi-states of generating units, transmission line contingencies can be considered in bulk system analysis. It is therefore important to understand which factors are integrated and which are not. Moreover, factors that are included in the system, need to realize how they impact on the system behaviour. The base case analysis of IEEE-RTS and other studies are done based on the following conditions.

- The step-down transformer at transformer stations are considered to be customer owned and the reliability indices are calculated at the high voltage Bus bars.
- Transmission line common mode failures are not taken into account.
- The economic priority order for load curtailment is utilized.
- System stations are not incorporated in the evaluation process.

The IEAR values for each load point [36] and corresponding priority order of the IEEE-RTS are shown in Table 2.1. The number of simulation samples must be sufficiently large

to obtain accurate results. Earlier studies [36] at the HL-II level show that reasonably accurate results can be obtained for the IEEE-RTS [36] with 500,000 samples. This sample size was used in the HL-II studies reported in this thesis.

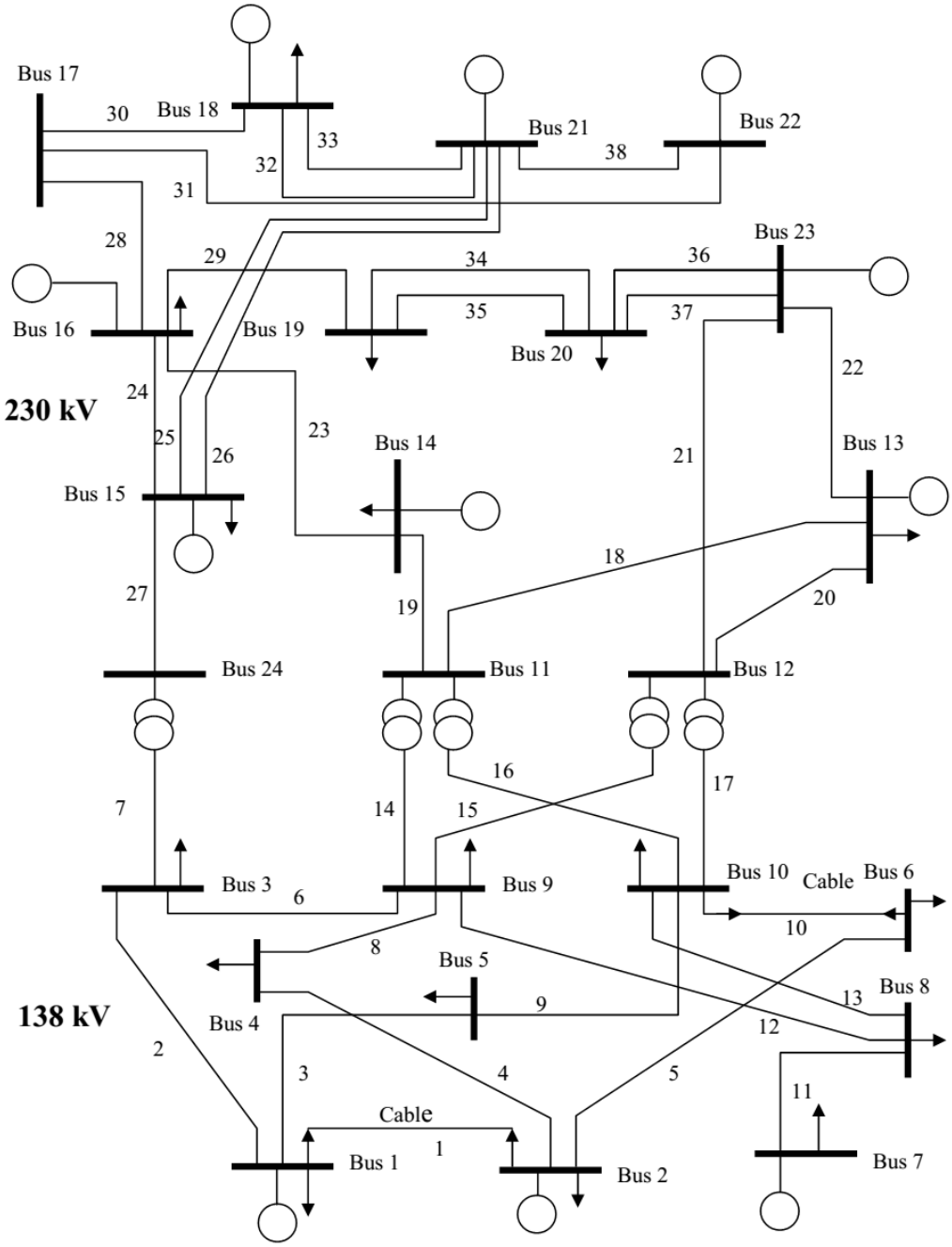

Figure 2.1: Single line diagram of the IEEE-RTS

Table 2.1: Bus IEAR values and priority order in the IEEE-RTS

Bus No.	IEAR ($/kWh)	Priority Order
1	6.20	1
2	4.89	9
3	5.30	8
4	5.62	3
5	6.11	2
6	5.50	4
7	5.41	5
8	5.40	6
9	2.30	16
10	4.14	10
13	5.39	7
14	3.41	14
15	3.01	15
16	3.54	13
18	3.75	11
19	2.29	17
20	3.64	12

The 20-step load model shown in Appendix is utilized to calculate the base case annual load point indices. The annual system indices and annual load point indices of the IEEE-RTS using the load model are shown in Table 2.2 and 2.3 respectively.

Table 2.2: Annual system indices for the IEEE-RTS

Indices	Annual value
ENLC (1/yr)	1.137
ADLC (hrs/disturbance)	11.445
EDLC (hrs/year)	13.018
PLC	0.00149
EDNS (MW)	0.19119
EENS (MWh/yr)	1674.80
EDC (K$/yr)	7067.65
BPII (MW/MW-yr)	0.05347
BECI (MWh/MW-yr)	0.58765
BPACI (MW/disturbance)	133.99
MBECI (MW/MW)	0.00007
SI (system minutes/yr)	35.26

The system EDLC of 13.018 hours/year and the EENS of 1674.80 MWh/year were obtained from the base case study of the IEEE-RTS. This system EENS is the summation of the load point EENS values shown in Table 2.3.

Table 2.3: Annual load point indices for the IEEE-RTS

Bus No.	PLC	ENLC (1/yr)	ELC (MW/yr)	EDNS (MW)	EENS (MWh/yr)
1	0.00000	0.00000	0.000	0.00000	0.000
2	0.00000	0.00080	0.024	0.00002	0.192
3	0.00000	0.00035	0.013	0.00001	0.099
4	0.00000	0.00000	0.000	0.00000	0.000
5	0.00000	0.00000	0.000	0.00000	0.000
6	0.00000	0.00075	0.055	0.00004	0.310
7	0.00000	0.00041	0.003	0.00000	0.015
8	0.00000	0.00002	0.000	0.00000	0.001
9	0.00083	0.65554	38.777	0.04890	428.392
10	0.00000	0.00321	0.161	0.00016	1.359
13	0.00000	0.00005	0.001	0.00000	0.010
14	0.00014	0.12319	7.366	0.00848	74.290
15	0.00047	0.37877	31.499	0.03795	332.480
16	0.00007	0.05775	2.076	0.00231	20.248
18	0.00002	0.02078	1.502	0.00156	13.661
19	0.00149	1.13619	69.293	0.08997	788.151
20	0.00004	0.03772	1.633	0.00178	15.590

It can be noted in Table 2.3 that the EENS at the Buses 9, 14, 15 and 19 contribute to 96% of the system index. It can be seen in Table 2.1 that these four buses have the lowest priority orders in the system. These load point indices are highly dependent on the load curtailment priority.

2.7 Summary

The basic features of the Monte Carlo simulation technique are discussed in this chapter. A non- sequential state sampling approach is described. This approach is used in the MECORE software introduced in this chapter. MECORE can be used for power system reliability evaluation

and reliability worth assessment. The capabilities and limitations of the software are also discussed. The MECORE software is used in this thesis to do the bulk system adequacy analysis. A wide range of HL-II reliability indices are discussed in this chapter. Two types of indices designated as load point and system indices are described. Overall system indices provide useful management indicators of system reliability.

The IEEE-RTS is utilized for bulk system reliability analysis in the work reported in the thesis is introduced. The IEEE-RTS 20-step load model is shown in Table A7 in the Appendix and this 20-step load model is used for a base case study. The annual system indices and annual load point indices obtained from the base case study are shown in Table 2.2 and Table 2.3 respectively. The results show that the load point indices are highly dependent on load curtailment philosophy. The annual system indices of a base case presented in Table 2.2 of this chapter are used as references in analyzing system conditions discussed in the following chapters.

3 DEVELOPMENT OF WIND AND SOLAR POWER MODELS FOR ADEQUACY ASSESSMENT OF BULK SYSTEMS

3.1 Introduction

Wind and solar energy generation are considered to be environment friendly and therefore, have received considerable attention in recent years. New technologies are continuously being developed to integrate wind and solar energy sources into the grid system and in stand-alone applications. Power generated from wind and solar energy sources varies randomly depending on the behaviour of the wind speed and solar irradiation, and their impacts on system performance can be very different than that of the conventional energy sources. It is important to develop accurate models to represent wind and solar energy sources and provide an appropriate methodology for power system planners to be able to carefully address the reliability issues associated with these energy sources.

Wind energy is converted to electric energy depending on the wind speed available at a particular time at the system location. Wind turbine generator converts kinetic energy of wind to electric energy. Three factors need to be considered to create an appropriate wind power model for bulk system analysis. Randomness of the wind speed at the generation site is the first factor. The variation in the power output of the generator is the second factor. The third factor is the random failure of the WTG characterized by its Forced Outage Rate (FOR) [19]. In this chapter, hourly wind speed data obtained from Environment Canada are converted to wind power using the wind power curve of the Wind Turbine Generator (WTG). A discrete probability distribution of the wind power at the WTG site is then created, and the number of discrete steps is reduced using an apportioning method to obtain a multi-state wind power model. Previous research showed that

FOR variations in WTG unit does not have a major impact on the system adequacy [19]. The FOR of WTG is taken as zero for simplicity in the analysis.

It is important to create accurate photovoltaic (PV) power generation models in order to analyze the impact of solar power on system adequacy. A three-step approach is also used to obtain the solar power model at a PV site. First, solar irradiation data needs to be collected for the particular site. The second step is the conversion of solar irradiation data to solar power using an appropriate relationship between them. The third step is the consideration of the FOR of the solar panel unit. Hourly solar irradiation data are not readily available for many sites. Monthly average data obtained for selected sites are processed to obtain hourly chronological data. A software program named SIPSREL+ [53] was used in this work to obtain hourly solar data for selected Saskatchewan sites. The solar irradiation data is then converted to solar power data. The FOR of PV units can be incorporated, but are ignored in this study as the FOR of PV units do not have significant impact on the overall system adequacy. The apportioning method is utilized to create a multi-state solar power model in a similar manner to that used to create the wind power model.

3.2 Developing a Wind Power Model

3.2.1 Wind Speed Data

Wind speed data for two Saskatchewan sites, Swift Current and Saskatoon, were obtained from Environment Canada [48], and used in the studies presented in this thesis. Twenty years of hourly wind speed data were available for these two sites. The mean and the standard deviation of the Swift Current wind speed data collected from 1 Jan, 1984 to 31 Dec, 2003 are 19.46 km/h and 9.7 km/h respectively. The mean and the standard deviation of the Saskatoon wind speed data collected from 1 Jan, 1986 to 31 Dec, 2005 are 15.35 km/h and 8.01 km/h respectively. Swift Current lies in the southwest part of the province, and is considered to be a site with a strong wind

resource. Most of the existing and proposed wind farms are in this region. On the other hand, the Saskatoon site has a relatively weak wind resource.

3.2.2 Conversion of Wind Speed to Wind Power

Availability of wind energy is dependent on the geographic site. The power output of a WTG is a function of the wind speed at the instant. The cut-in wind speed, rated wind speed and cut-out wind speed are the three operational parameters of a WTG that influence its power output. A WTG begins generating power at its cut-in wind speed. Rated power is generated from a WTG when the wind speed is between the rated wind speed and the cut-out wind speed. AWTG is shut down for safety purpose at its cut-out wind speed.

WTG power output can be obtained using (3.1).

$$P(SW_t) = \begin{cases} 0 & 0 \le SW_t < V_{ci} \\ (A + B \times SW_t + C \times SW_t^2) \times P_r & V_{ci} \le SW_t < V_r \\ P_r & V_r \le SW_t < V_{co} \\ 0 & SW_t \ge V_{co} \end{cases} \quad (3.1)$$

Here V_{ci}, V_r,V_{co} and P_r, are the cut-in wind speed, the rated wind speed, the cut-out wind speed and the rated power output of the wind turbine generator respectively [49]. The constants A, B and C can be calculated from (3.2).

$$A = \frac{1}{(V_{ci}-V_r)^2}\left\{V_{ci}(V_{ci}+V_r) - 4V_{ci}V_r\left[\frac{V_{ci}+V_r}{2V_r}\right]^3\right\} \quad (3.2)$$

$$B = \frac{1}{(V_{ci}-V_r)^2}\left\{4(V_{ci}+V_r)\left[\frac{V_{ci}+V_r}{2V_r}\right]^3 - (3V_{ci}+V_r)\right\}$$

$$C = \frac{1}{(V_{ci}-V_r)^2}\left\{2 - 4\left[\frac{V_{ci}+V_r}{2V_r}\right]^3\right\}$$

The power curve shown in Figure 3.1 represents the relationship between wind speed and WTG power output expressed in (3.2).

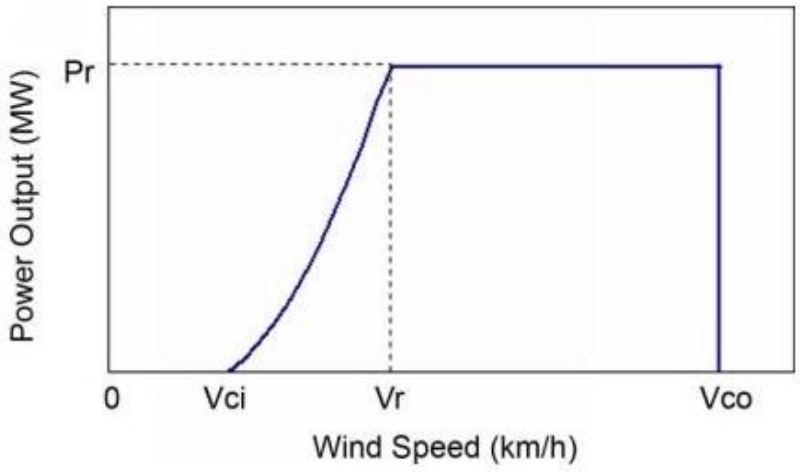

Figure 3.1: Wind turbine generator power curve

The data used for the WTG parameters; the cut-in speed, rated speed and cut-off speed are 14.4km/h, 36 km/h and 80km/h respectively in the studies presented in this thesis. The hourly WTG power output data is obtained from the twenty years of hourly wind speed data using (3.1).

3.2.3 Developing the Wind Power Model

A discrete probability distribution of the wind power output at a geographic site is created using the 20 years of wind power data obtained as described in the previous section. The method is described below.

1. The wind power data is expressed in per unit of the rated power output.
2. The number of intervals or discrete steps is calculated using Sturge's rule [2].
3. The data is grouped into the different intervals, and the power output state of each interval is represented by the mid-point value of the interval.
4. The total number of the power output data in each interval is counted to obtain the frequency of each power output state.
5. The frequency of each output state is divided by the total number of data points to calculate the probability of each state.

The discrete probability distributions of wind power obtained following the above steps for Swift Current and Saskatoon locations are shown in Figure 3.2. The data used for the WTG cut-in speed, rated speed and cut-off speed were 14.4 km/h, 36 km/h and 80 km/h respectively. These distributions can be expressed as a Capacity Outage Probability Table (COPT) [1]. Using this approach, the two COPTs were created for the two sites, Swift Current and Saskatoon separately. Table 3.1 shows the two COPTs with 18 states determined using Sturge's rule [2]. Each capacity interval in the wind power models is 6.25% of the rated WTG capacity.

Table 3.1: Capacity outage probability tables for the Swift Current and Saskatoon wind sites

Swift Current		**Saskatoon**	
Mean Wind Speed = 19.46 km/h		**Mean Wind Speed = 15.35 km/h**	
Capacity Outage (%)	**Probability**	**Capacity Outage (%)**	**Probability**
0	0.0578	0	0.0216
3.125	0	3.125	0
9.375	0.0165	9.375	0.008
15.625	0	15.625	0
21.875	0.0275	21.875	0.0116
28.125	0.0142	28.125	0.0084
34.375	0.0140	34.375	0.0055
40.625	0.0354	40.625	0.0193
46.875	0	46.875	0
53.125	0.0447	53.125	0.0250
59.375	0.0506	59.375	0.0309
65.625	0.0001	65.625	0
71.875	0.0512	71.875	0.0390
78.125	0.0678	78.125	0.0465
84.375	0.0673	84.375	0.0516
90.625	0.0821	90.625	0.066
96.875	0.1658	96.875	0.1662
100	0.3052	100	0.5006

Figure 3.2 shows that the capacity outage probability distribution for both Swift Current and Saskatoon sites are discontinuous because of limited wind data collection. It can be seen that the Swift Current site has a stronger wind power profile than that of the Saskatoon site. The expected

power outputs at the Swift Current and Saskatoon sites are 22.88% and 12.39% respectively. The probability of 100% outage for Swift Current is 0.3052 which is lower than the Saskatoon 100% outage probability of 0.5006. The probability of generating rated capacity at the Swift Current site is 0.0578, which is higher than 0.0216 from the Saskatoon site.

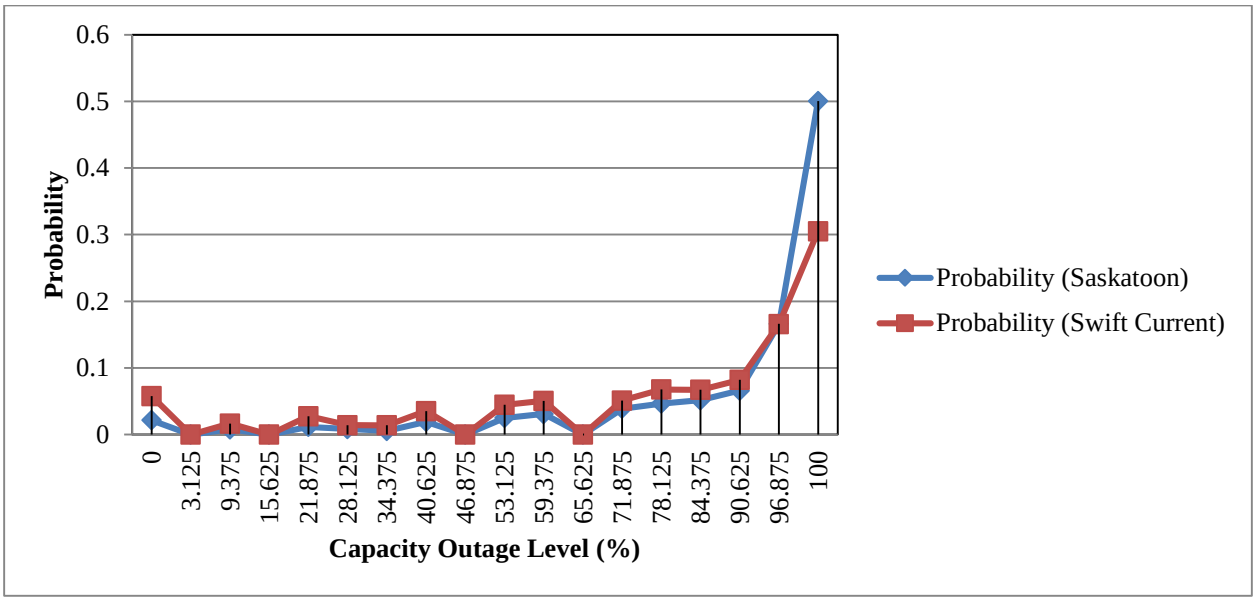

Figure 3.2: Capacity outage probability for two different wind resources

3.2.4 Developing an Appropriate Multi-state Wind Power Model

A generating unit can reside in more than two states (up state, down state) in its operating history [45, 50]. These states are referred to as derated states [45, 50]. A reasonable number of derated states are necessary to represent the wind power model for adequacy analysis as wind power output capacity state varies in a wide range. It has been determined in previous research [19] that a five state wind power model is reasonable to carry out adequacy analysis in the MECORE software [19]. Studies have shown that wind power models with five or more states provide similar results [19]. In this thesis, five state models are used to represent both the Swift Current and Saskatoon wind resources.

Different methods, such as the pre-convolution capacity rounding method [51] and apportioning method [19], have previously been used to reduce the number of capacity states in wind power models. As pre-convolution capacity rounding methods create new capacity states, the adequacy evaluation results are often inaccurate. The apportioning technique is considered to be more accurate than the rounding technique. The 18-state COPT shown in the Table 3.1 is reduced to a five state model using the apportioning method [19] and shown in Table 3.2 for both the Swift Current and Saskatoon wind sites. As mentioned earlier, the FOR of the WTG is not considered. Figure 3.3 shows the pictorial representations of the discrete 5-state probability distributions of wind power outages for the two sites.

Table 3.2: Two five state WTG COPTs for two different sites without considering FOR

Swift Current		**Saskatoon**	
Capacity Outage (%)	**Probability**	**Capacity Outage (%)**	**Probability**
0	0.07155	0	0.02805
25	0.06470	25	0.03118
50	0.10633	50	0.06124
75	0.22233	75	0.16730
100	0.53530	100	0.71244

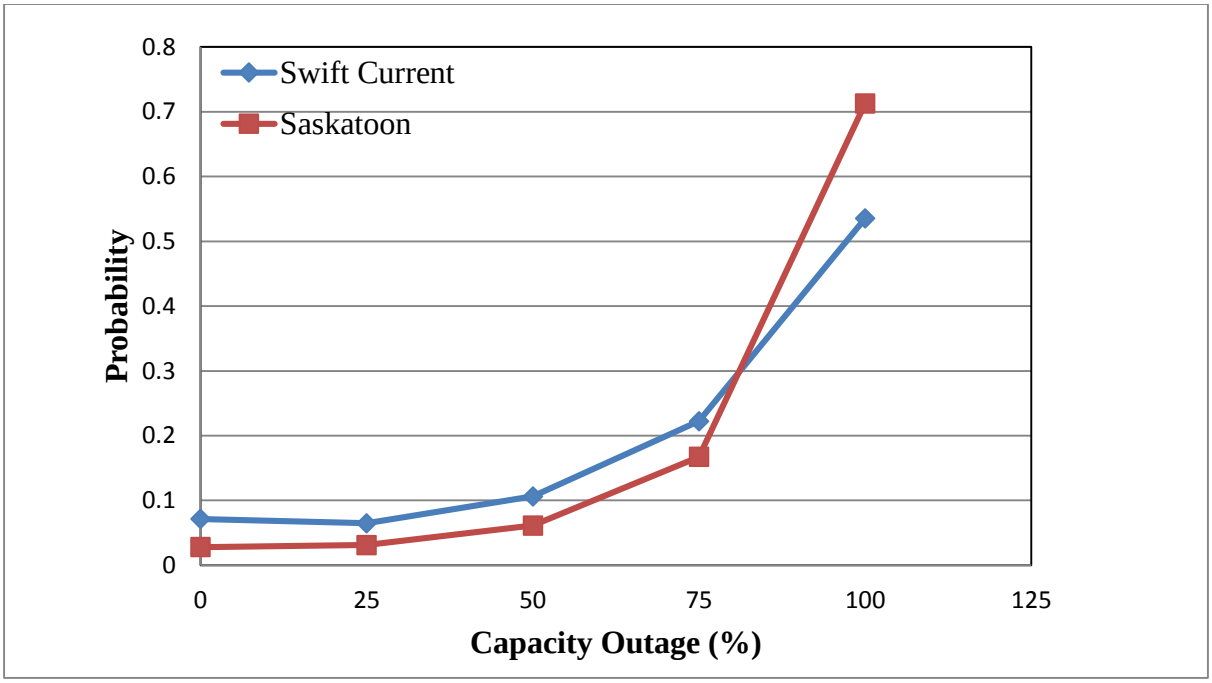

Figure 3.3: Five state capacity outage probability for two different wind resources

3.3 Developing the PV Power Model

3.3.1 Photovoltaic Conversion System

Photovoltaic is the combination of two words. The Greek word “Photo” stands for light and the “Volta” comes from electricity inventor Alessandro Volta [34]. A Photovoltaic system includes the whole process of converting solar light to electricity and supplying it to the load points [34]. Solar panels are created by connecting solar cells in series and parallel. Solar panels are similarly connected to create an array. A photovoltaic conversion system (PVCS) consists of a number of photovoltaic arrays.

Power generation from a PV array depends on the solar irradiation at the site and the solar cell efficiency. PV array arrangement and the DC to AC conversion to the grid are other important factors affecting the power output of PVCS [34].

3.3.2 Solar Irradiation Data

Solar power output from a PV device depends on the amount of solar irradiation on the PV cell. Modeling of solar radiation at the earth surface is very complicated due to a large number of variables related to the earth's atmospheric conditions. Radiation outside the earth atmosphere is called extraterrestrial radiation [34]. The average value of the extraterrestrial radiation is 1367 (W/m^2), and is known as the solar constant [52]. The portion of solar radiation received by the PV array to generate electricity is known as global radiation, which depends on weather variations, earth's latitude, season, time of day, array surface angle, etc. The global radiation at the PV array surface can be divided into direct and diffuse components, where direct radiation is the component that directly reaches the surface, and diffuse radiation is the component that reaches the array surface through scattering factors such as water vapour and clouds [34].

As hourly time resolution is generally used in adequacy evaluation of power system, hourly solar irradiation data are required at the particular PV installation sites. Hourly solar irradiation data, however, are not readily available in many locations which leads to simulating the hourly solar radiation data for a good number of years utilizing generation of synthetic data. The SIPSREL+ [53] software developed at the University of Saskatchewan can generate synthetic hourly solar radiation on a horizontal surface on earth using a simulation method from monthly average solar irradiation data. A stochastic probability transformation of the clearness index is utilized to get a Gaussian random variable [53]. This Gaussian random variable has the same mean and variance for each month. In Auto Regressive Moving Average (ARMA) model (1, 0) this variable is utilized to calculate the hourly solar radiation data on a horizontal surface [19]. Two steps are followed in SIPSREL+ to generate the hourly average solar radiation data for a particular site [53]. In the first step, daily average solar irradiation data is simulated for a PV site using

monthly average wind speed, ambient temperature and solar irradiation data. Hourly mean solar irradiation data is then generated for a year (8760 hours) in the second step using the daily irradiation data using the daily values generated in the first step. In this thesis, twenty years of solar irradiation data were generated for the Swift Current site using SIPSREL+.

3.3.3 PV Power Modeling

The solar power output from the solar panel depends on the efficiency of the solar cells, solar irradiation and other factors. There are different ways to model the solar power output from a photovoltaic system. In this thesis, an analytical method is utilized to model solar power. In an analytical model the output power relies on solar cell efficiency and radiation on the solar cell. The power output of a PV array can be determined from the relation between solar radiation and PV output shown in Figure 3.4. This relation is mathematically expressed in (3.5 – 3.7) [55].

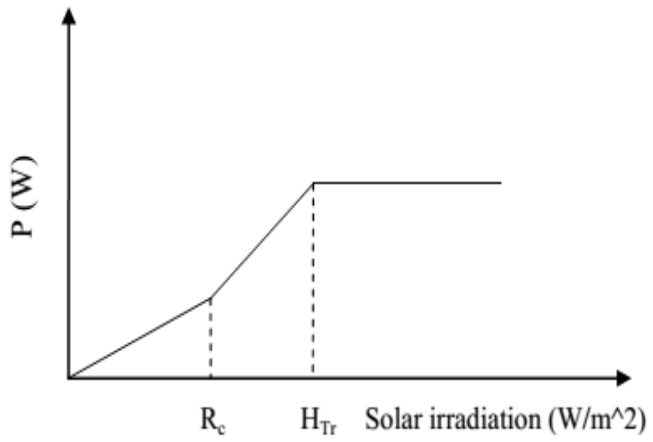

Figure 3.4: Relation between solar irradiation and PV power output [34].

$$\eta = \frac{\eta_c}{R_c} \times H_T \qquad 0 \leq H_T < R_c \qquad (3.3)$$

$$\eta = \eta_c \qquad R_c \leq H_T \qquad (3.4)$$

$$P = P_{sn} \times \frac{H_T^2}{H_{Tr} \times R_c} \qquad 0 \leq H_T < R_c \qquad (3.5)$$

$$P = P_{sn} \times \frac{H_T}{H_{Tr}} \qquad R_c \leq H_T < H_{Tr} \qquad (3.6)$$

$$P = P_{sn} \qquad H_T \geq H_{Tr} \qquad (3.7)$$

Here,

P = the PV power output (W)

H_T = hourly solar radiation (W/m^2)

H_{Tr} = solar radiation in a standard environment set as 1000 (W/m^2)

R_c = a certain radiation point set as 150 (W/m^2)

η = efficiency of PV module

η_c= rated module efficiency

Twenty years of hourly solar irradiation data generated for the Swift Current site was converted to power using the above equations. The following procedure is used to create a COPT of a PV array.

1. The solar power data is expressed in per unit of the rated solar power output.
2. The number of intervals or discrete steps is calculated using Sturge's rule [2].
3. The data is grouped into the different intervals, and the solar power output state of each interval is represented by the mid-point value of the interval.
4. The total number of the solar power output data in each interval is counted to get

the frequency of each solar power output state.

5. The frequency of each output state is divided by the total number of data points to compute the probability of each state.

The COPT of a PVCS created for the Swift site following the above steps, is shown in Table 3.3.

Table 3.3: COPT of a PVCS installed at the Swift Current site

Capacity Outage (%)	**Probability**
0	0.001
3.125	0.0043
9.375	0.0074
15.625	0.0113
21.875	0.0143
28.125	0.0174
34.375	0.0194
40.625	0.0220
46.875	0.0252
53.125	0.0275
59.375	0.0317
65.625	0.0380
71.875	0.0421
78.125	0.0484
84.375	0.0393
90.625	0.0248
96.875	0.1486
100	0.4773

As PVCS are only capable of generating power during the daytime, a daytime COPT can be developed to appropriately model the contribution of these intermittent power sources. The duration of daylight time varies seasonally depending on the geographical location. Table 3.4 show the daytime COPT of a PVCS at the Swift Current location assuming a daylight time of 12 hours.

Table 3.4: Daytime COPT of a PVCS installed at the Swift Current site

Capacity Outage (%)	Probability
0	0.0019
3.125	0.0078
9.375	0.0137
15.625	0.0209
21.875	0.0264
28.125	0.0322
34.375	0.0358
40.625	0.0405
46.875	0.0465
53.125	0.0507
59.375	0.0586
65.625	0.0701
71.875	0.0777
78.125	0.0860
84.375	0.0671
90.625	0.0420
96.875	0.2047
100	0.1172

The comparison between Tables 3.3 and 3.4 shows that the 12-hour daytime model in Table 3.4 has a lower probability of zero power output than that of the 24-hour model shown in Table 3.3. This is due to absence of PV power during the nighttime.

3.3.4 Developing an Appropriate Multi-state PV Model

PV power output varies in a wide range due to variation in solar irradiation. A PVCS should be represented by a model with a reasonable number of derated states in order to accurately conduct adequacy assessment using the MECORE software. Reference [19] showed that a solar power model with five or more states provide similar results. Therefore, a five state solar model is considered to represent PVCS in this study. The COPT shown in Table 3.3 and Table 3.4 were reduced to five state models using the apportioning method [19], and are shown in Table 3.5. The

24-hour day and nighttime PVCS model is compared with the daytime model using the 5-state representation in Figure 3.5.

Table 3.5: Two five state COPTs for two different solar contribution using Swift Current data

Day and nighttime COPT		**Daytime COPT**	
Capacity Outage (%)	**Probability**	**Capacity Outage (%)**	**Probability**
0	0.01661	0	0.03066
25	0.05927	25	0.10942
50	0.11317	50	0.20879
75	0.16396	75	0.28641
100	0.64699	100	0.36472

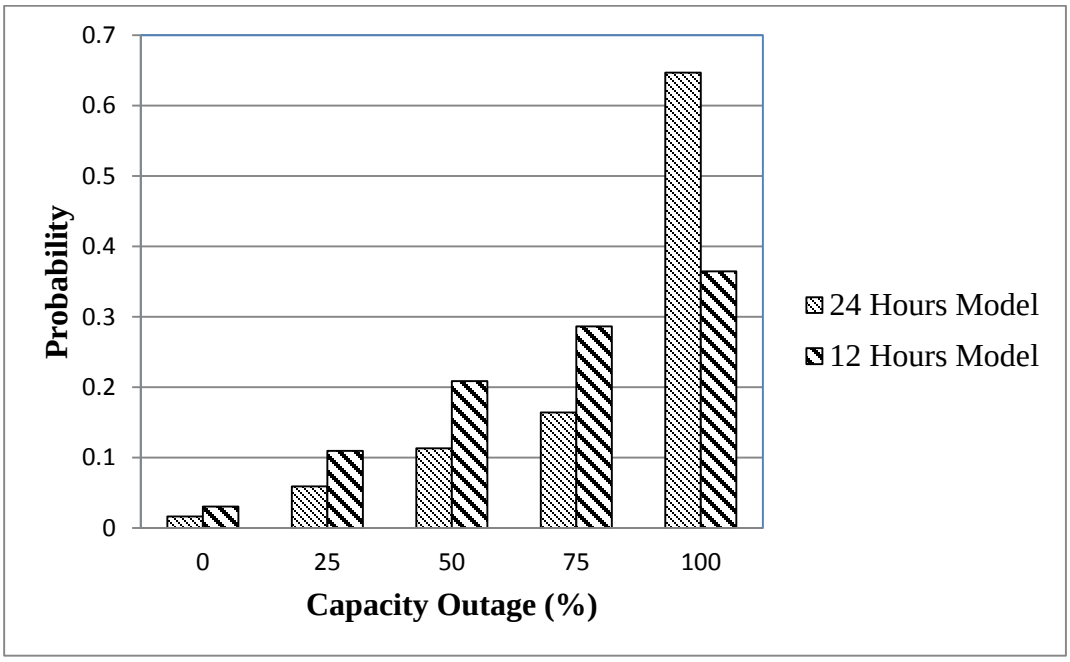

Figure 3.5: A Comparison of the 12-hour (daytime) and 24-hour (day-and-nighttime) PV Power Models

3.4 Summary

This chapter presents the methodology used to develop the wind and solar power models for reliability evaluation. Hourly available wind speed data for the Swift Current and Saskatoon locations and the generation of synthetic data for the two sites are discussed. Modeling a wind

turbine generator considering its operating parameters to get the power output using the wind speed as the input data is explained. The SIPSREL+ software is introduced in this chapter which was used to create hourly synthetic solar radiation data using monthly average values for the Swift current location. An analytical technique was introduced to calculate the solar power output from the hourly solar irradiation data.

The method to develop the discrete probability distribution of the wind power and solar power are illustrated with examples of Swift Current and Saskatoon data. These wind and solar power models are reduced to 5-state models using an apportioning technique to simplify the computation.

The daytime and 24-hour PV power model are developed to examine the contribution of PV sources to overall system reliability. These models are used for further system analysis in a later chapter.

4 WIND INTEGRATED BULK SYSTEM ADEQUACY ANALYSIS

4.1 Introduction

Power systems planners routinely expand their generation systems by adding appropriate types and capacities of generation to the existing system in time to replace retiring units and to meet growing demands. It is possible that a power system with adequate generation capacity may have unacceptable system reliability due to inadequate transmission capacity to deliver available power to the major load points. System planners therefore also routinely upgrade and expand transmission capability to adequately carry generated power to the load points with growing demands. Over the past decade, wind power has been one of the most important generation sources added to power systems. Power system planners therefore need the ability to assess the cost and reliability impact of adding wind resources to the system. This analysis includes assessing the capabilities of the transmission lines to adequately deliver the fluctuating power due to the wind resources to continuously meet the load demands.

Most electric utilities do not use probabilistic methods to evaluate the adequacy of their transmission systems. Many utilities use a deterministic "N-1" criterion that requires the system to be in no difficulty when single major transmission line or generating unit is on forced outage. Probabilistic methods are more capable than existing deterministic methods to incorporate the random nature of power delivery requirements in wind-integrated power systems [36]. Appropriate probabilistic models to represent wind energy sources, and techniques to incorporate these models in composite system reliability are presented in this thesis. A Monte Carlo simulation approach using state sampling and enumeration techniques are used in this work to analyze wind integrated bulk system adequacy.

The contribution of wind power to bulk system reliability not only depends on the capacity of the wind source but also on the network location where the wind power is injected into the system. It is important to consider that some buses have relatively weak transmission line support compared to others, and system planners need to be able to evaluate the reliability impact of adding wind farms at appropriate buses in the system. Wind farm owners build their farms where they find good wind resources and they don't necessarily consider the network configuration of the system. A relatively weak wind resource may be utilized and connected to a network location with a relatively strong transmission capability from a network point of view. Therefore, the ability to analyze the system at the HL-II level is essential to observe the contributions of the transmission system to the system indices as well as to the load point indices. It is equally important in system planning to evaluate the locational impacts of new generating capacity based on network topology.

4.2 Impact of Transmission Outages on Bulk System Adequacy

4.2.1 HL-II Evaluation of the IEEE-RTS

The IEEE-RTS is used as the test system in this study. The single line diagram is shown in Figure 2.1 and the system data is provided in the Appendix.

The reliability of the system was evaluated using the MECORE software for two cases: (a) without considering the transmission system, and (b) considering the transmission system. The generation system was considered in both cases. Table 4.1 shows the system reliability indices for the two cases.

Table 4.1: The IEEE-RTS reliability indices with and without considering the transmission system

Annual System Indices	**Considering the Generation Outages Only**	**Considering Both Generation & Transmission Outages**
Expected Number of Load Curtailments (ENLC) in occ./ year	1.03015	1.13760
Average Duration of Load Curtailment (ADLC) in hrs/disturbance	11.95543	11.44315
Expected Duration of Load Curtailment (EDLC) in hrs/ year	12.31638	13.01818
Probability of Load Curtailments (PLC)	0.00141	0.00149
Expected Demand Not Supplied (EDNS) in MW	0.17423	0.19120
Expected Energy Not Supplied (EENS) in MWh/ year	1526.21746	1674.87666
Expected Damage Cost (EDC) in k$/ year	6440.63771	7067.97898
Bulk Power-Interruption Index (BPII) in MW/MW- year	0.04728	0.05349
Bulk Power/Energy Curtailment Index (BECI) in MWh/MW- year	0.53551	0.58768
Bulk Power-Supply Average MW Curtailment Index (BPACI) in MW/disturbance	130.80208	133.99492
Modified Bulk/Energy Curtailment Index (MBECI) in MW/MW	0.00006	0.00007
Severity Index (SI) in system minutes/ year	32.13089	35.26056

Table 4.1 clearly shows that transmission line outages affect the reliability indices. The results show that the system reliability decreases when the transmission system is considered in the evaluation. The effects are, however, not very large in the IEEE-RTS due to the fact that the IEEE-RTS has a relatively strong transmission system.

4.2.2 Peak Load Carrying Capability of the Bulk System

The peak load of a power system generally increases with time. The peak load of the IEEE-RTS is 2850 MW. A study was done by varying the system peak load, from 2800 MW to 3000 MW in 50 MW steps, in order to assess the effect of the system peak load on the system adequacy. The system EDLC was evaluated for the two cases described in the previous section, i.e. (a) without considering the transmission system outages, and (b) considering the transmission system outages in the evaluation. The system EDLC values obtained from the MECORE software are shown in Table 4.2.

Table 4.2: Variation of the system EDLC with the system peak load evaluated with and without considering transmission line outages

Peak Load (MW)	**EDLC in hrs/yr (Considering Generation Outages Only)**	**EDLC in hrs/yr (Considering Both Generation and Transmission Line Outages)**
2800	8.85	9.77
2850	12.32	13.02
2900	16.02	18.01
2950	21.21	23.93
3000	28.47	30.37

Table 4.2 shows that the system EDLC increases significantly with increase in the system peak load. A comparison of the results for the two cases shows that the EDLC values are higher

when the transmission outages are considered in the evaluation. The difference between the EDLC results for the two cases quantifies the contribution of the transmission system to the reliability index. It should be noted that the difference in the EDLC index increases as the peak load is increased. This is because the relatively strong IEEE-RTS transmission system becomes weaker as the peak load is increased, and therefore, the impacts of the transmission outages are more significant.

The EDLC of the IEEE RTS, with 3405 MW generating capacity and 2850 MW peak load is 12.32 hrs/yr when only the generation outages are considered in the system analysis. In other words, the system can carry a peak load of 2850 MW while meeting an EDLC criterion of 12.32 hrs/yr. The peak load carrying capability was also calculated at this criterion when both the generation and transmission line outages were considered in the evaluation. The results are shown in Table 4.3. There is a 10.8 MW reduction in the peak load carrying capability of the system due to transmission line outages.

Table 4.3: Peak load carrying capability with and without considering transmission line outages

Study Type	**Peak Load Carrying Capability (MW)**
Considering the Generation Outages Only	2850.0
Considering Both the Generation and Transmission Line Outages	2839.2

4.3 Impact of Wind Resource Strength on Bulk System Adequacy

Bulk system adequacy is highly dependent on the wind characteristics of the wind farms connected to the power system. Wind resources in the Swift Current and Saskatoon regions are considered in the study to analyze the impact of wind resource strength on bulk system adequacy. The wind power models developed for the two locations are presented in Table 3.2 of Chapter 3.

The Swift Current site with a mean wind speed of 19.46 km/hour has a wind resource stronger than that of Saskatoon which has a mean wind speed of 15.35 km/hour.

It is assumed that a 400 MW Swift Current wind farm is connected to Bus 1 of the IEEE-RTS. The 400 MW wind power addition to the 3405 MW system results in a wind penetration of 10.5%. The system peak load is 2850 MW. The system EDLC was found to be 8.80 hrs/yr using the MECORE software. A similar study was carried out considering the 400 MW wind farm to have Saskatoon wind characteristics instead of Swift Current. The system EDLC in this case was found to be 10.58 hrs/yr.

Studies were also conducted to evaluate the impact of increasing wind power penetration on bulk system adequacy. The system EDLC values were evaluated assuming that the wind penetration at Bus 1 increased from 10.5% to 20%, 30% and 40% considering the wind regimes for both the Swift Current and Saskatoon sites. The corresponding wind capacities for the four penetration levels are 400 MW, 850 MW, 1460 MW and 2270 MW respectively. The results are shown in Figure 4.1.

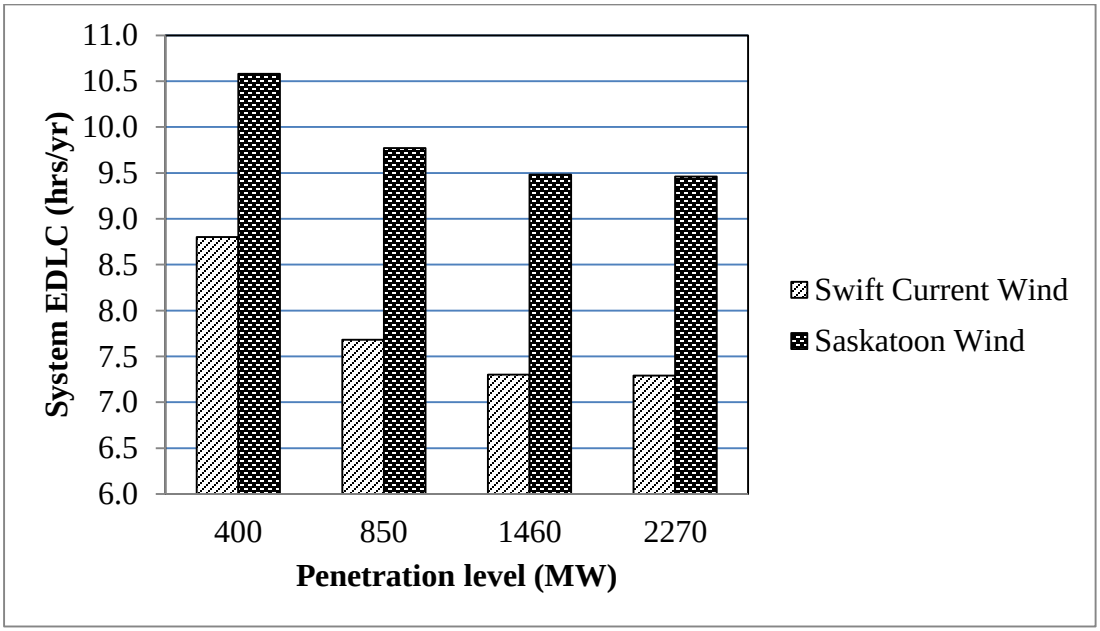

Figure 4.1: Impact of wind resource strength and wind power growth on bulk system adequacy

Figure 4.1 shows that the EDLC decreases (the system reliability increases), with the increase in wind power penetration. It can however be seen that the incremental reliability benefit decreases with increasing wind penetration, and the benefit tends to saturate at a certain high penetration level. Figure 4.1 shows that the reliability contribution of the 400 MW wind farm with the Swift Current wind regime is significantly higher than that of the wind farm with the Saskatoon wind regime. It can be observed from Figure 4.1 that even if the capacity of the Saskatoon wind farm were infinite, its reliability contribution would be less than that of the 400 MW Swift Current farm.

4.3.1 Comparison of the Reliability Impact of a Wind Resource on Different System Configurations

The previous study was conducted on the IEEE-RTS which has a relatively weak generation system and a strong transmission network. The results show that the transmission outages have less impact on the reliability indices than generation outages. In order to create a different system configuration, the IEEE-RTS was modified by increasing the system peak load to 3420 MW and the total generation to 3946 MW. The Modified IEEE-RTS (MRTS) was created to provide a system which has a relatively weak transmission system, and operates relatively close to the capacity limits under peak load conditions. The MRTS resembles many power systems in which transmission expansion lags generation expansion implemented in response to load growth. In reality, a power system that is initially like the IEEE-RTS, changes to MRTS with passage of time unless the transmission network undergoes timely upgrades and expansion. Studies were carried out to compare the reliability impacts of wind power injection in the two systems, the IEEE-RTS and the MRTS that have very different generation and relative transmission capabilities. Figure 4.2 shows the EDLC for the two systems considering three scenarios; (i) no

wind, (ii) a 400 MW wind farm with the Swift Current wind resource connected at Bus 1, and (iii) 5% load growth with the 400 MW wind farm.

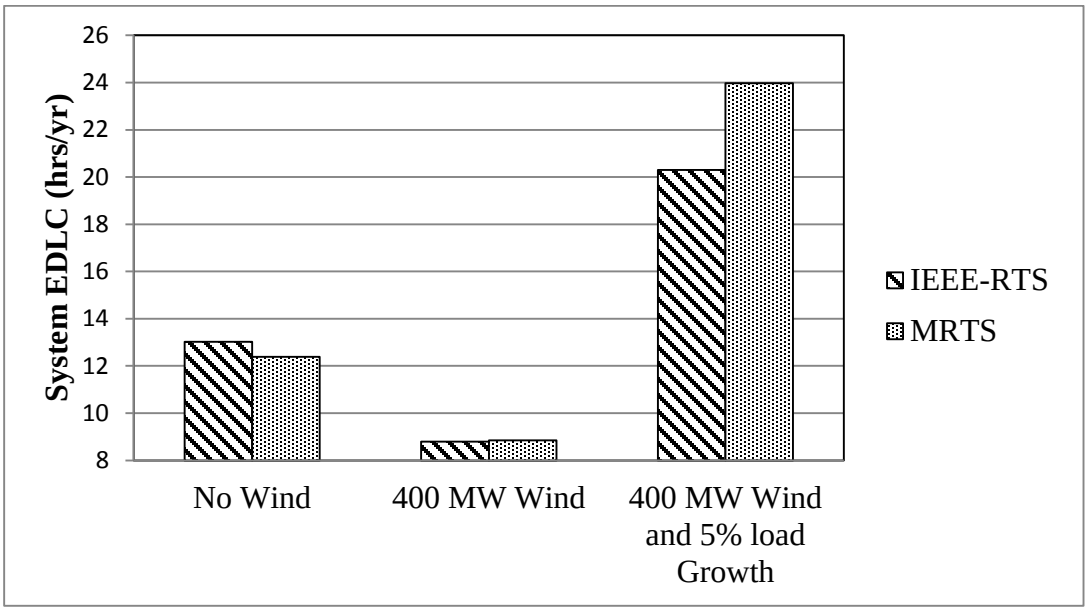

Figure 4.2: Wind injection impact on the bulk system reliability of two different system scenarios

Figure 4.2 shows that the EDLC of the IEEE-RTS and MRTS are 13.02 hours/year and 12.40 hours/year correspondingly with no wind, and the MRTS is a somewhat more reliable system than the IEEE-RTS. The reliability of the MRTS becomes slightly lower than that of the IEEE-RTS when a 400 MW wind farm with the Swift Current wind resource is included at Bus 1 in both systems. The reliability of the MRTS becomes significantly lower than that of the IEEE-RTS with the wind injection when the peak load is increased by 5%. This is for the most part because the transmission system of the MRTS is relatively weaker than that of the IEEE-RTS.

4.4 Impact of a Wind Injection Point in the Grid Network

It is discussed earlier that wind integrated bulk system adequacy is dependent not only on the strength of the wind resources, but also on the transmission network configuration. Wind farm

owners are primarily interested in the revenues resulting from wind energy sales, and therefore, invest in wind farm installations in geographic locations with good wind regimes. They are less interested in the network configuration of the system, and reliability contribution to the overall system. Power system planners, on the other hand, are concerned about the reliability impact on the system contributed by wind power additions. At the same time, they are also concerned about the associated system costs and environmental effects. It is therefore important for system planners to determine the significance of the network buses in terms of interconnecting wind farms for overall benefits, and to quantify the benefits of interconnection at different bus locations. This section presents a study that assesses the reliability benefit of connecting wind resource at different network buses in the transmission network.

A 400 MW farm with the Swift Current wind regime is used for this study. Two different wind injection points, Bus 1 and Bus 7 of the IEEE-RTS, are utilized. In the first case, the 400 MW wind farm is connected to Bus 1 of the IEEE-RTS. In the second case, the same wind farm is connected to Bus 7. MECORE is used to simulate the system for each case and obtain the reliability indices. The system EDLC is 8.80 hrs/yr and 12.40 hrs/yr when the wind farm is connected to Bus 1 and Bus 7 respectively. It can be seen that the same wind source provides different levels of reliability of the bulk system. Connecting the wind farm at Bus 1 provides higher reliability benefit than connecting at Bus 7. If both the buses are located in regions with similar wind resources, then the Bus 1 location should be selected for wind farm installation. The reason is that Bus 1 is more capable than Bus 7 of delivering power to the load points. It can be observed from Figure 2.1 that the wind power injected at Bus 1 can be transmitted through three different transmission lines, Line 1, Line 2 and Line 3. On the other hand, wind power injected at Bus 7 can only be transmitted

through Line 11. The probability of outage or congestion of Line 11 is the main reason for the reduced reliability benefit from wind power connected at Bus 7.

A study was also conducted to investigate the reliability benefit of connecting a wind resource at the two different network buses considering increases in the system peak load. The system peak load was increased from 2800 MW to 3000 MW in 50 MW steps. The EDLC results are shown in Figure 4.3. The EDLC of wind with connected at Bus 7 is greater than the EDLC with wind at Bus 1 for the entire range of system peak loads. It can be seen that the difference increases with increase in the system load.

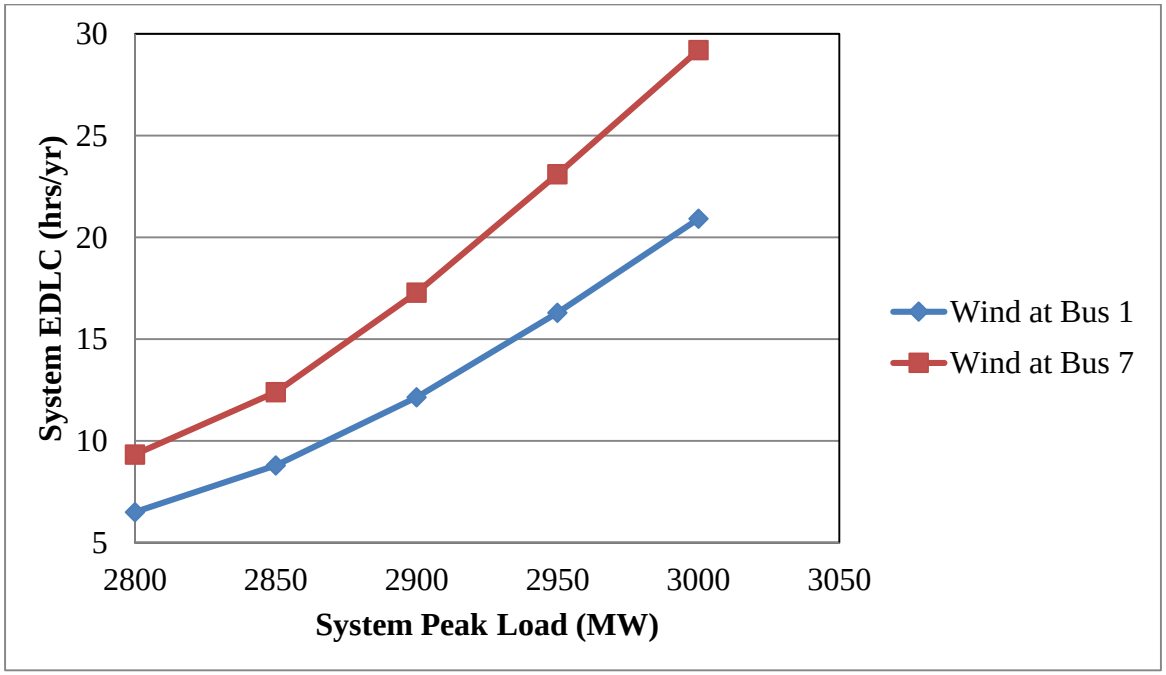

Figure 4.3: Bulk system reliability impact of a wind injection point in the IEEE-RTS network

4.5 Wind Diversity Impact on Bulk System Adequacy

Many electric power utilities have experienced a significant amount of wind energy growth in their systems within the last decade, and this trend is expected to continue in the next decade.

The growth of wind power involves installations of wind turbines in areas where high wind speed is available for successful operation. As an example, many wind farms are located in the southwest corner of Saskatchewan province in Canada.

Wind power generation varies randomly and is utilized by the system whenever available. Rapid increments of wind power in a particular area with strong wind resource will cause the transmission system to become congested and therefore limits the reliability benefits to the system. Another reason for reduced benefits is that the power outputs of all the wind turbine generators depend on the same wind regime. A potential solution to this problem is to distribute the wind farms to multiple areas with diverse wind profiles. Studies done at the HL-I [56] and HL-II [36] level show the reliability benefit of distributing wind power installations to multiple areas with diverse wind profiles. It should, however, be noted that diversifying wind resource can require selection of new wind farm installation sites that have weaker wind resources than the existing wind farm sites, or are in remote areas that involve extensive transmission additions.

Power output from two wind farms are correlated to some extent unless the distance between them is significantly large. It is proved that there is a relation between correlation and distance. The wind speed correlation between two sites decreases as the distance between them increases [36]. The correlation between wind farms at different sites can and should be considered in system modeling for adequacy assessment. The random failure behaviour of a component within a power system can be represented by a uniform distribution where component outages are independent. Conventional generating unit model and independent wind farms model follow this procedure. Partially dependent wind farms are taken into consideration by dividing the uniformly distributed random numbers between [0, 1] into two clusters [36]. The first cluster of random numbers represents the conventional generating units or independent wind farms and the second

cluster random numbers represent correlated wind farms. Two correlated wind farms are modeled by generating two sets of random numbers for each wind farm and creating clusters of correlated and uncorrelated random numbers in the state sampling simulation process. MECORE was modified in [36] to incorporate wind speed correlation between multiple wind farms using this approach to evaluate the bulk system adequacy indices. The cross correlation coefficient of wind speeds between the two wind farms lies between 0 to 1, and can be obtained from historical data. A high value indicates that the wind speeds between the farms are highly correlated. For instance, cross correlation coefficients of 1 means the wind farms are fully dependent on each other.

A study was initially carried out using the IEEE-RTS to investigate the impact of wind injection at different bus locations without considering wind diversity on the adequacy of a power system. Two wind farms connected to Bus 2 and Bus 5 are considered in this study. Bus 2 is connected to 192 MW of conventional generation, 97 MW active load and three transmission lines connected to Buses 1, 4 and 6. The load curtailment priority for Bus 2 is nine, and its IEAR is 4.89 $/kWh. Bus 5 is connected to 71 MW of active load, and two transmission lines that connect to Bus 1 and Bus 10. Bus 5 is not directly connected to generation plants. The load curtailment priority order is two, and its IEAR is 6.11 $/kWh. Wind farm capacity of 400 MW with the Swift Current wind profile was considered for three different cases; (1) all wind capacity connected to Bus 2, (2) all wind capacity connected to Bus 5, and (3) wind capacity divided equally between the two buses. The cross correlation between the wind speeds at the two farms is 1 in the third case. The system EDLC obtained for a range of peak loads are shown in Table 4.4.

Table 4.4: System EDLC with 400 MW wind capacity at Bus 2, at Bus 5 and at both the buses simultaneously

System Peak Load (MW)	System EDLC (hrs/yr) when 400 MW Wind Capacity Connected to		
	Bus 2	Bus 5	Bus 2 & Bus 5 (equally divided)
2800	6.51	6.54	6.48
2850	8.82	8.86	8.78
2900	12.18	12.22	12.13
2950	16.34	16.39	16.28
3000	20.97	21.04	20.87

Table 4.4 shows that the system reliability is improved when the wind capacity is divided equally between the two buses when compared to the first two cases where all the wind capacity was connected either at Bus 2 or Bus 5. The reduction of stress on the associated network is the main reason for the reliability improvement.

Another study was done to assess the impact of wind diversity on the bulk system adequacy. The 400 MW wind capacity with Swift Current wind profile was equally divided between Bus 2 and Bus 5 in this study. Three cases of wind diversity considered in this study are; (1) the wind farms are fully dependent, (2) the wind farms are moderately dependent with a cross correlation coefficient of 0.5, and (3) the wind farms are totally independent. A fourth case is considered where the 400 MW wind capacity is equally divided between Bus 2, Bus 5 and Bus 4, and the three wind farms are totally independent. Table 4.5 shows the results from the four different cases for a range of peak loads.

Table 4.5: Reliability impact of diversifying 400 MW wind capacity connected to the IEEE-RTS

System Peak Load (MW)	EDLC (hrs/yr) with Two Wind Farms			EDLC (hrs/yr) with 3 Wind Farms
	Totally Dependent	Moderately Dependent	Totally Independent	Totally Independent
2800	6.48	6.13	5.76	5.46
2850	8.78	8.32	7.86	7.46
2900	12.13	11.50	10.85	10.20
2950	16.28	15.49	14.65	13.89
3000	20.87	19.89	18.86	18.42

The results in Table 4.5 show that reliability benefits rise with the decrease in correlation between the two wind farms, or in other words, the reliability benefits increase with the increase of diversity between the wind farms. As mentioned earlier, the diversity between wind farms generally increases when the distance between them is increased. It can be seen from Table 4.5 that the largest reliability benefits are obtained when wind farms are totally independent. In actual applications, the wind farms connected to a power system are neither totally independent nor totally dependent.

A comparison of results for Case 3 and Case 4 shows that there is further reliability benefit when the wind farms are distributed at three different locations. Figure 4.4 shows the EDLC of the two cases as a function of the system peak load for comparison. It can be seen that the system EDLC is reduced for the fourth case with the three independent wind farms. This is mainly due to reduced stress on the associated network as discussed earlier.

In the above studies the wind farms connected to the IEEE-RTS have equally good wind regimes. In most pragmatic scenarios, new wind installation sites chosen to create diversity will generally have relatively lower wind regimes compared to the existing wind resources or will involve considerable transmission costs. Power system planners should therefore conduct a comprehensive reliability evaluation incorporating wind speed correlation between wind farms,

wind resource strength, transmission requirements on wind locations in order to get maximum reliability benefits for the system.

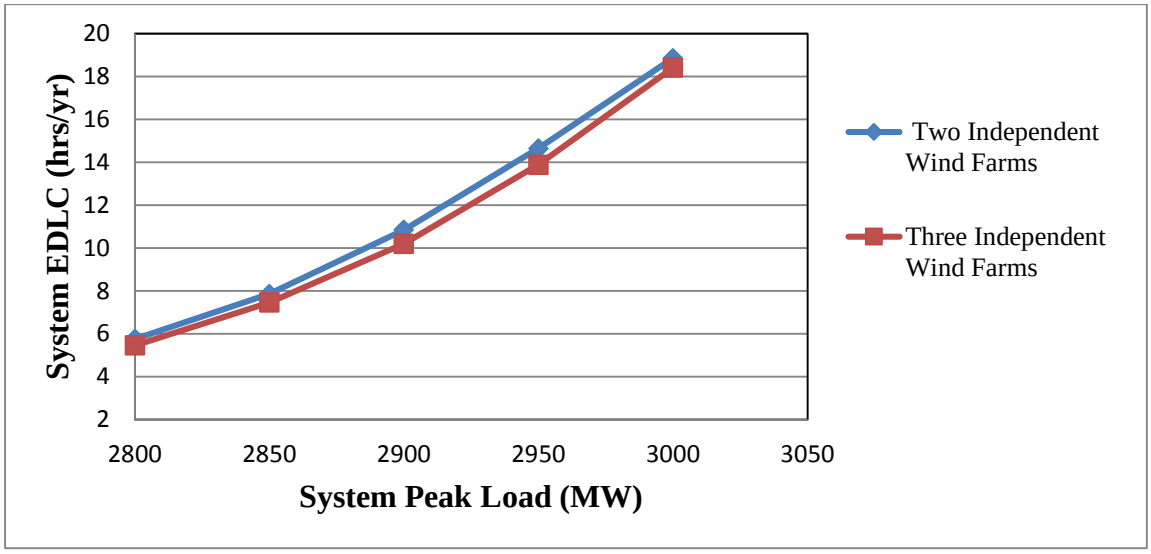

Figure 4.4: EDLC variations for independent wind farms at IEEE-RTS

4.6 Wind Energy Reliability Benefit and Reliability Worth Analysis

Wind farm installation in the power industry is rapidly growing as an alternate source of electric energy. The amount of wind energy reliability benefit and the customers' cost savings due to wind energy from the wind farm are important aspects to consider. The selection of a wind farm installation site is very important as it affects the amount of wind energy contribution to the system as well as the customers' outage cost savings. Wind reliability benefit and customer outage cost reduction due to wind energy added depend on many factors, such as the strength of the wind resource at the site, wind farm injection point in the system network, cross correlation of wind speeds at the different wind farm locations. In this thesis these three important factors are investigated to analyze the wind energy reliability benefit to the system and the associated outage cost savings due to wind energy addition.

The wind energy contribution to the system can be expressed in terms of the Expected Wind Reliability Benefit (EWRB) and is calculated using Equation 4.1. The Expected Damage

Cost (EDC) due to energy not supplied to the customers is calculated by multiplying the average system Interrupted Energy Assessment Rate (IEAR) by the system Expected Energy Not Supplied (EENS). The IEAR for the IEEE-RTS is 4.22 $/kWh, and this index measures the customer outage loss as a function of energy not supplied for the entire system or for particular sectors within the system.

$$EWRB = EENS_{NW} - EENSw \quad (4.1)$$

where, $EENS_{NW}$ = Overall Expected Energy Not Supplied to the System excluding wind

$EENS_w$ = Overall Expected Energy Not Supplied to the System considering wind

Customer' outage Cost Savings (CCS_w) due to wind energy supplied can be calculated using equation 4.2.

$$CCS_w = EDC_{NW} - EDC_w \quad (4.2)$$

where, EDC_{NW} = Overall Expected Damage Cost of the System excluding wind

EDC_w= Overall Expected Damage Cost of the System considering wind

The $EENS_{NW}$ and EDC_{NW} of the IEEE-RTS are 1674.88 MWhr/yr and 7067.98 k$/yr respectively as shown in Table 4.1. The EWRB and CCS_w are evaluated in the following section to quantify the wind energy contribution to the system and customers' outage cost savings due to wind energy supplied.

4.6.1 Impact of Network Location of Wind Injection on the Wind Energy Reliability Benefit and Reliability Worth

It has been mentioned earlier that the contribution of wind energy and customers' outage cost savings due to wind energy provided depend on the network connection point of the wind farm. A study was carried out to investigate the impact on bulk system adequacy and reliability worth of connecting wind capacity to a power system at different network bus locations. A 400

MW wind farm using Swift Current wind data was first considered to be connected to Bus 1of the IEEE-RTS, and the MECORE software was used to assess the system $EENS_W$ and EDC_W. The study was repeated with the wind farm connected to Buses 2, 5 and 7 respectively. Table 4.6 shows the $EENS_W$ and EDC_W when the wind farm is separately considered at the four different buses. It can be seen from Table 4.6 that the indices are very close for first three cases of Buses 1, 2 and 5. The results are significantly different for the fourth case where the farm is connected to Bus 7. Wind penetration at Bus 7 provides $EENS_W$ of 1591.89MWh/yr which is significantly higher than the EENSw when the wind farm is connected to the other buses. The EDC_W follows the same trend as $EENS_W$ because EDC_W is calculated by multiplying the average system IEAR with the overall system $EENS_W$. The EDC_W 6717.78 k$/yr while a 400 MW wind connected to Bus 7 is higher than that of the other cases. Single line transmission at Bus 7 is the reason for the relatively high EDC_W.

Table 4.6: System $EENS_w$ and EDC_w of the IEEE-RTS with a 400 MW wind farm connected at different buses

Cases	**$EENS_W$ (MWh/yr)**	**EDC_W (k$/yr)**
Wind at Bus 1	1102.12	4650.94
Wind at Bus 2	1103.15	4655.30
Wind at Bus 5	1107.46	4673.48
Wind at Bus 7	1591.89	6717.78
No Wind	1674.88	7067.98

The EWRB were also calculated for the IEEE-RTS using Equation 4.1 considering the 400 MW wind farm connected to Buses 1, 2, 5 and 7. The results are shown in Figure 4.5. Among the four cases, wind injection at Bus 1 provided the maximum wind energy contribution to the system with an EWRB of 572.76MWh/yr. The lowest wind energy contribution was obtained when the

wind farm was connected to Bus 7. The EWRB in this case was 82.98MWh/yr due to a single line transmission connection at this bus.

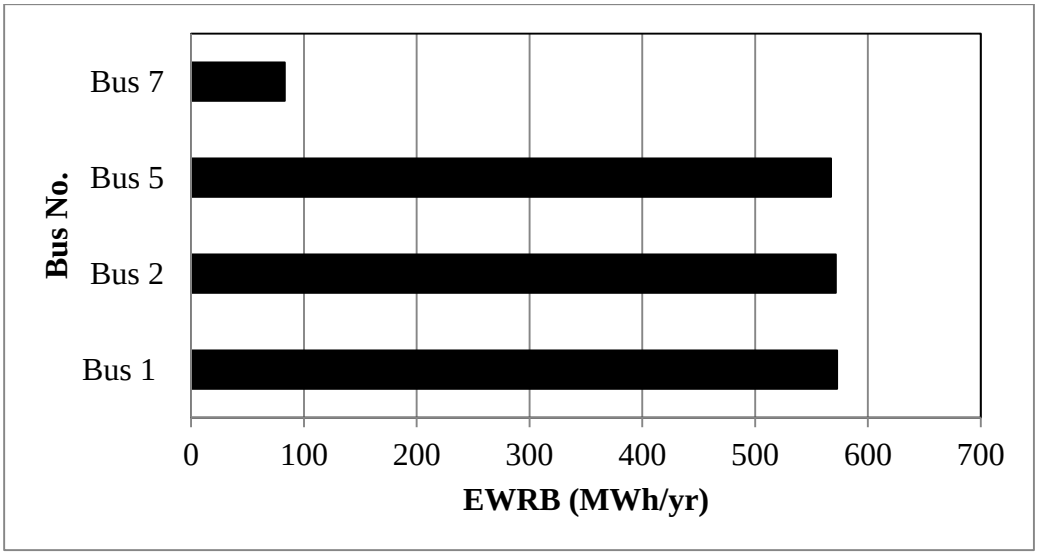

Figure 4.5: Expected Wind Reliability Benefit (EWRB) with a 400 MW wind farm connected at Buses 1, 2, 5 and 7 of the IEEE-RTS

The customer outage cost savings due to wind energy supplied (CCS_w) were calculated using Equation 4.2, with a 400 MW wind farm connected to Buses 1, 2, 5 and 7 respectively. Figure 4.6 shows wind penetration at Bus 1 provided the highest CCS_w of 2417.04 k$/yr among the four cases. The lowest CCS_w of 350.20 k$ among the four cases occurred with the wind farm connected at Bus 7.

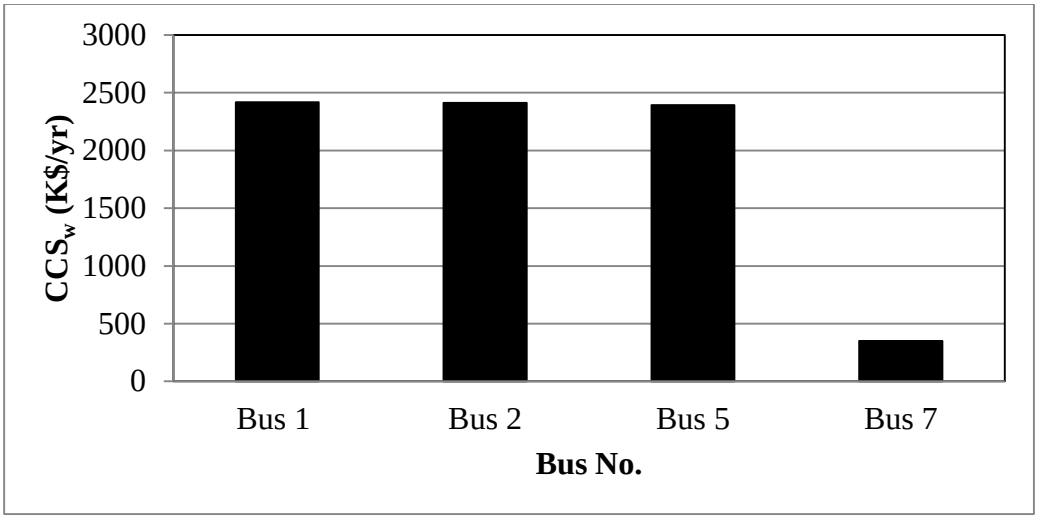

Figure 4.6: Customer outage cost saving due to wind energy supplied (CCS_w) with a 400 MW wind farm connected at Buses 1, 2, 5 and 7 of the IEEE-RTS

The results show that Bus 7 is the worst location among the four buses to connect the wind farm because of the reduction in cost saving as well as poor wind energy contribution to the system due to the single transmission line available at this bus to deliver the wind energy. It is therefore important to consider the system configuration when deciding new wind installations, or upgrades the system configuration in preparation for the new wind installations in order to maximise the wind energy utilization and outage cost benefits from the wind additions to the system.

4.6.2 Impact of the Wind Regime on the Wind Energy Reliability Benefit and Reliability Worth

A study was carried out to study the impact of the strength of the wind regime on the bulk system adequacy and reliability worth. A 400 MW wind farm was assumed at Bus 1 of the IEEE-RTS considering two different cases of wind profile data; (1) Swift Current wind profile, and (2) Saskatoon wind profile. The MECORE software was used to assess the system $EENS_w$, EDC_w, EWRB and CCS_w. In both cases, a constant system peak of 2850 MW is considered. Table 4.7 displays the indices for two cases. The results show that the Swift Current wind resource provides

higher system reliability, wind energy reliability benefit and reliability worth than the Saskatoon wind resource.

Table 4.7: Impact of wind regime strength on the system reliability indices

Wind Regime	$EENS_W$ (MWh/yr)	EDC_W (k$/yr)	EWRB (MWh/yr)	CCS_w (k$/yr)
Swift Current	1102.12	4650.94	572.76	2417.04
Saskatoon	1344.01	5671.74	330.87	1396.24

4.6.3 Impact of Wind Diversification on the Expected Wind Reliability Benefit and Reliability Worth

Wind energy diversification can play a significant role in energy contribution and customer outage cost saving. A study was done to observe wind diversity impact on the bulk system reliability worth and reliability benefit. A wind farm capacity of 400 MW with the Swift Current wind profile was connected to the IEEE-RTS considering three different cases in this study; (1) all wind capacity connected to Bus 2, (2) all wind capacity connected to Bus 5, and (3) wind capacity divided equally between the two buses. The cross correlation between the wind speeds at the two farms is 1 in the third case. All three cases were simulated using the MECORE software to assess the system $EENS_W$, EDC_W, EWRB and CCS_w, which are shown in Table 4.8.

Table 4.8: System $EENS_W$, EDC_W, EWRB and CCS_w with 400 MW wind capacity at Bus 2, at Bus 5 and at both the buses simultaneously

Wind Farm Connected to	$EENS_W$ (MWh/yr)	EDC_W (k$/yr)	EWRB (MWh/yr)	CCS_w (k$/yr)
Bus 2	1103.15	4655.30	571.73	2412.68
Bus 5	1107.46	4673.48	567.42	2394.50
Bus 2 & Bus 5 (equally divided)	1102.85	4654.04	572.03	2413.97

Table 4.8 shows the wind energy utilization and the associated bulk system reliability. The expected wind reliability benefit and the reliability worth are improved when the wind capacity is divided equally between the two buses when compared to the first two cases where all the wind capacity was connected either at Bus 2 or Bus 5. As mentioned earlier, the reduction in stress on the associated network is the main cause of the reliability enhancement.

An additional study was carried out where the 400 MW wind capacity with the Swift Current wind profile was equally divided between Bus 2 and Bus 5. Three cases of wind diversity considered in this study are; (1) the wind farms are fully dependent, (2) the wind farms are moderately dependent with a cross correlation coefficient of 0.5, and (3) the wind farms are totally independent. Table 4.9 shows the $EENS_{W,}$ $EDC_{W,}$ EWRB and CCS_w for the three different cases. It is seen from the results in Table 4.9 that the bulk system reliability worth and energy reliability benefit improve with the increase in diversity or a decrease in the cross correlation coefficient of wind speeds between the two wind farms.

Table 4.9: Reliability cost/worth impact of diversifying 400 MW wind capacity connected to the IEEE-RTS

Wind Diversity Cases	**$EENS_W$ (MWh/yr)**	**EDC_W (k$/yr)**	**EWRB (MWh/yr)**	**CCS_w (k$/yr)**
Totally Dependent	1102.85	4654.04	572.03	2413.97
Moderately Dependent	1037.05	4376.35	637.83	2691.63
Totally Independent	972.42	4103.60	702.46	2964.38

4.7 Conclusion

The impact of generation and transmission line outages on the reliability indices is discussed at the beginning of this chapter. The bulk system reliability considering both the generation and transmission constraints is reduced when compared to the system reliability considering only generation constraints and an ideal transmission system. The peak load carrying capability of the IEEE-RTS is reduced by 10.80 MW when the transmission constraints are added to the generation constraints in the reliability evaluation.

Studies were carried out to assess the impact of wind resource strength on system adequacy. The Swift Current and Saskatoon wind resources were used to conduct this analysis. The Swift Current location has a stronger wind resource and therefore provides better reliability benefits than Saskatoon regime when connected to the same network connection point of a power system. A study was conducted by injecting different wind penetration levels at the same network bus of the IEEE-RTS. Increased wind penetration provided better system adequacy but at certain penetration levels such as 1460 MW, 2270 MW the reliability benefit ceased and saturated.

The impact of wind power and power system configuration on bulk system adequacy was analyzed by carrying out comparative studies on the MRTS and the IEEE-RTS. The MRTS is slightly more reliable but has a weaker transmission system than the IEEE-RTS. The MRTS becomes slightly less reliable than IEEE-RTS when a 400 MW Swift current wind resource is added. The reliability of the MRTS becomes significantly lower than that of the IEEE-RTS when the peak load is increased by 5% in addition to 400 MW wind. The reason for this is that the transmission system for MRTS is relatively weaker than that of the IEEE-RTS.

The wind injection point in the grid is an important factor for power system planners. Two network locations (Bus 1 and Bus 7) were chosen to examine the impact of the wind connection

point in the network. The system peak load was varied and a 400 MW Swift Current wind farm was injected at Bus 1 and Bus 7 separately. The wind farm connected to Bus 7 provided lower system reliability benefits than that at Bus 1 for the entire range of system peak load. This was basically due to single line configuration at Bus 7 which held back the improvement in system reliability.

Diversification of wind energy is discussed in this chapter. Wind capacity distributed between two wind farms provides better reliability than the same total capacity at a single wind farm. The impact of wind power diversity in two wind farms was analyzed using the IEEE-RTS. The studies show that the reliability increases as the diversity between the wind farms increase. The study also showed that wind capacity distributed at three independent sites provided better reliability than wind capacity diversified at two independent sites for equal amounts of total wind capacity. This is due to further reduced stress on the system transmission network.

Wind energy reliability benefit and customer outage cost saving due to wind energy provided were analyzed based on three different factors; (i) network location of wind penetration, (ii) wind regime and (iii) wind power diversification. Wind energy reliability benefit and customer outage cost saving was higher when the wind farm was connected to Bus 1 because it is a better configured bus compared to other buses based on network topology. Bus 7 is connected to a single transmission line, and therefore resulted in a poor energy contribution as well as poor customers' outage cost savings than the other buses. Energy reliability benefit and reliability worth were also evaluated based on different wind regimes. The Saskatoon wind regime provided poor wind energy contributions and lower customers' outage cost savings than the Swift Current wind regime. Customer outage cost saving due to wind energy contribution was examined based on wind energy diversification as well. Wind reliability benefits improved for two diversified wind farms over

having all the wind power in one place. It was also shown in another study, that customer outage cost saving improves with decrease in the cross correlation coefficient of the wind speeds at different wind farms.

5 SOLAR INTEGRATED BULK SYSTEM ADEQUACY ANALYSIS

5.1 Introduction

The application of solar energy to meet electrical energy needs is steadily increasing due to growing public awareness on environmental pollution from conventional energy sources. Solar energy is generally available everywhere, and is a potential source of electricity in areas that are remotely located from major power grids. The applications in electric power systems are also increasing as an important generation component in the renewable energy portfolio as PV costs continue to decrease. Significant increases in PV penetration in power systems can have substantial impacts on power system adequacy. The impact of different factors of PV energy on generation system adequacy has been studied in the past [34]. Relatively little work has been done considering PV energy in bulk system adequacy. A growing number of electric utilities are considering PV integration in their bulk systems. It is challenging for power system engineers to completely comprehend the impacts of PV energy bulk power system due a large number of influencing variables, such as weather dependent variability of PV energy, types of solar cells and their performance characteristics. These factors make solar integrated bulk system adequacy assessment different from conventional assessments, and therefore, new research in this area is important to provide useful evaluation methods for power system planners.

It is important for power system engineers to appreciate the reliability advantage of solar farms over wind farms, or the vice versa in bulk system planning. Solar or wind farm establishment depends on key factors such as the availability of wind or solar irradiation on the specific site. The impacts on cost and reliability of the bulk system are important indicators in justifying the investments in the two renewable energy sources. In this chapter a comparison between wind

integrated bulk system adequacy and solar integrated bulk system adequacy is done in order to identify appropriate renewable energy options for bulk system reliability.

5.2 Adequacy Analysis Based on Installed Solar Capacity Variations

The capacity of a solar farm connected to a power system can have significant influence on the overall bulk system reliability. Solar radiation in the Swift Current region is used in this study to evaluate the impact of installed solar capacity on bulk system adequacy. The five state whole day (including day and night) solar power model developed in Table 3.5 was used to examine the reliability contribution of adding PV generation to the bulk system. The IEEE-RTS is utilized in this study.

The bulk system EDLC of the IEEE-RTS with a peak load of2850 MW is 13.02 hrs/yr. A 400 MW Swift Current solar farm is assumed to be connected at Bus 1 of the IEEE-RTS. A 400 MW solar power addition to the 3405 MW system causes 10.5% solar penetration. It is assumed that the solar farm consists of a number of identical PV arrays of BP4175T. The electrical characteristics of a BP 4175T array are shown in the Appendix [54]. The system EDLC obtained by MECORE in this case is 9.88 hrs/yr. The system EDLC decreased by 24% by adding 10.5% PV power to the bulk system.

The system EDLC was also evaluated for a range of system peak loads assuming the solar capacity at Bus 1 to be increased from 10.5% to 20%, 30% and 40% using the same Swift Current solar resource. The corresponding solar capacities are 850 MW, 1460 MW and 2270 MW respectively. The results are shown in Figure 5.1

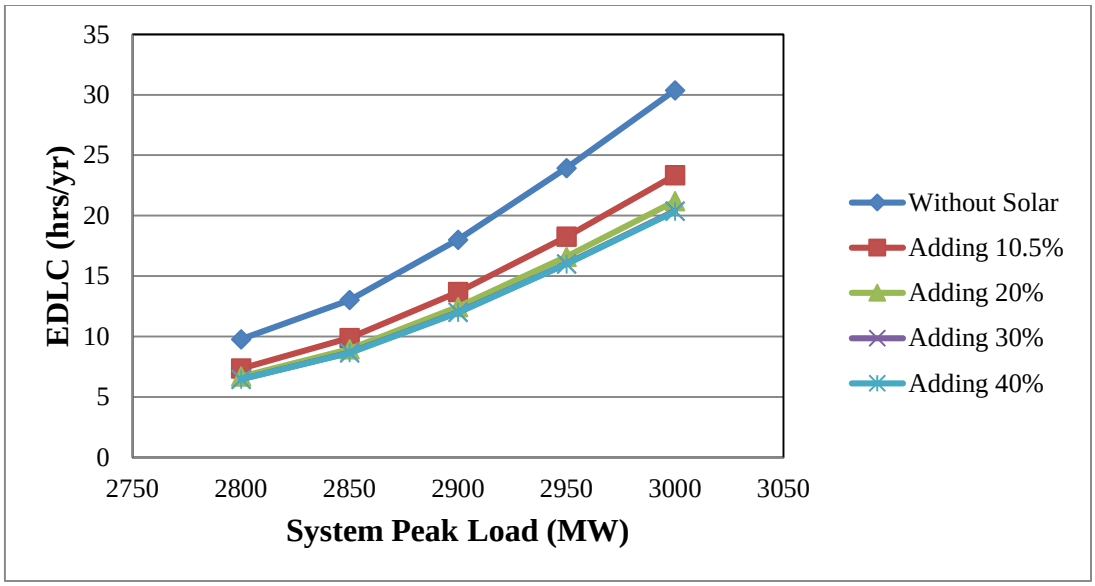

Figure 5.1: EDLC variation for different solar capacities and peak load levels

Figure 5.1 shows that the EDLC increases with the peak load increases for each solar penetration level. At a given peak load, adding PV capacity to the system decreases the system EDLC. At a system peak load of 2850 MW, the system EDLC decreases from the without solar case by around 31%, 33%, and 34% when 850 MW, 1460 MW and 2270 MW of solar power are installed at Bus 1 respectively. The system EDLC reaches a saturation level at higher level penetrations such as 30% and 40% solar penetration. This clearly indicates that there is no reliability benefit of increasing installed solar capacity after a certain penetration level.

The Increase in Peak Load Carrying Capability (IPLCC) was calculated and is shown in Figure 5.2 for the different installed solar capacity levels. The EDLC of 13.02 hrs/yr obtained without adding PV to the system is taken as the reliability criterion in assessing the PLCC.

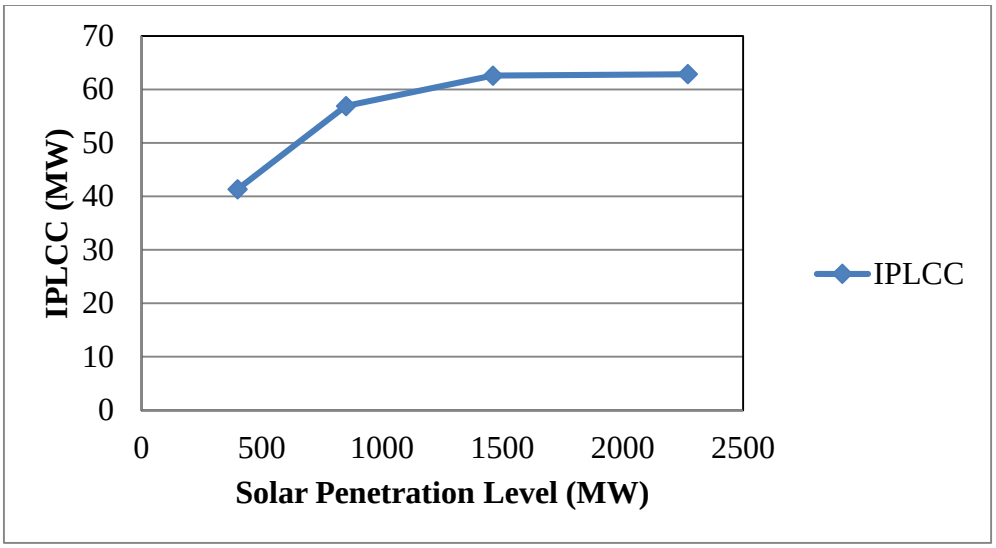

Figure 5.2: System IPLCC for different level solar penetrations connected to Bus 1

Figure 5.2 shows the IPLCC increases with solar penetration. Figure 5.2 also shows that the incremental reliability benefit decreases with increasing solar injection. The Incremental reliability benefit tends to saturate at a certain penetration level where after which there is no further benefit in increasing solar capacity. It can be seen that at about 1500 MW installed capacity or about 30% solar penetration the IPLCC tends to saturate around 63 MW.

5.3 Daytime Solar Contribution to the Bulk System Reliability

As PV systems are not expected to contribute during the nighttime, a study was carried out to investigate the daytime contribution of solar power to bulk system reliability. The daytime solar irradiation data for the Swift Current location was used to create PV models in this study. Figure 5.3 shows the capacity probability distribution for both the daytime solar model (12-hour) and the whole day (24-hour) solar model.

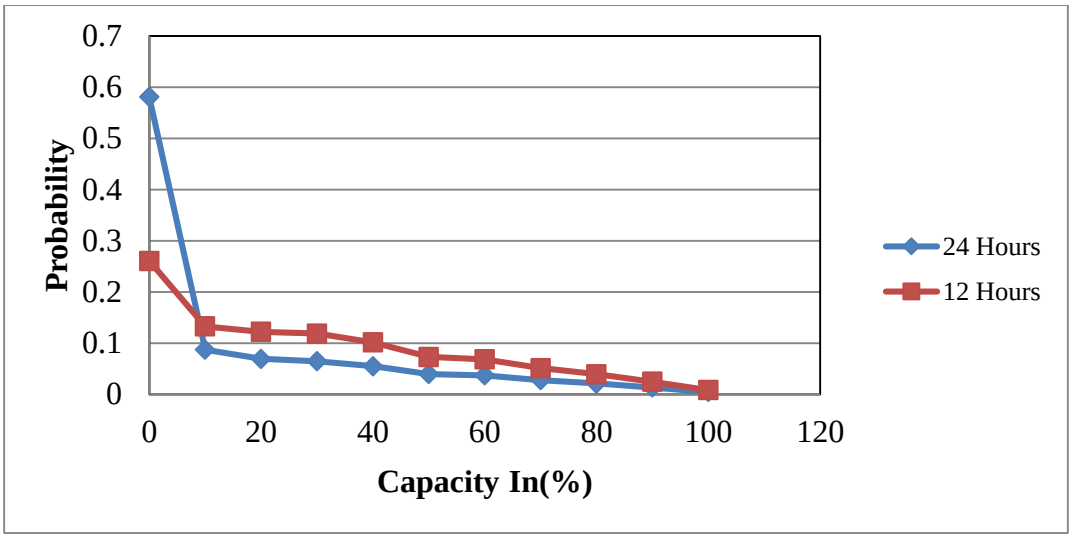

Figure 5.3: Probability distribution of PV Capacity for 24-hour and 12-hour models

An HL-II study was done on the IEEE-RTS considering 400 MW of solar capacity at Bus 1. The daytime reliability contribution of solar power on the bulk system uses the daytime model shown in Chapter 3. Figure 5.4 shows the resulting EDLC considering the daytime or 12-hour PV model, the whole-day or 24-hour PV model, and the base case without considering PV in the system. The contribution of solar power on bulk system adequacy is the reduction in EDLC from the base case where solar power was not considered.

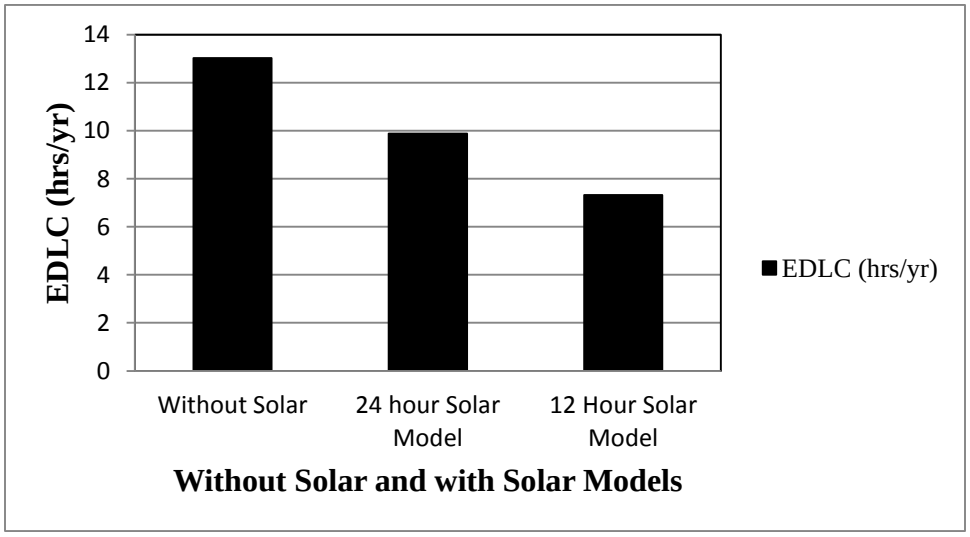

Figure 5.4: Bulk System risk evaluation of the IEEE-RTS using daytime and whole day solar models

5.3.1 Comparison of Solar Contribution Impact on Different System Configurations

The impact of solar contribution on the configuration of a power system is analyzed in this section. Studies were done to compare the reliability impact of daytime solar contributions in the IEEE-RTS and the MRTS. Their generation and transmission configuration and capabilities are notably different. The MRTS has a relatively weak transmission system compared to the IEEE-RTS. Figure 5.5 shows the EDLC for the two systems considering no solar and 400 MW of solar capacity with the Swift Current resource connected at Bus 1. The system peak load is 2850 MW. A third case was considered with 5% growth in the peak load with the solar farm. The IEEE-RTS and MRTS have EDLC of 13.02 hours/year and 12.40 hours/year respectively without solar power, which indicates that the MRTS is a more reliable system than the IEEE-RTS. Figure 5.5 shows that system reliability improves slightly for the IEEE-RTS compared to the MRTS when 400 MW of solar power is connected at Bus 1 in both systems. The reliability of the MRTS drops significantly more than that of the IEEE-RTS when the system peak load is raised by 5%. The relatively weak transmission system in the MRTS is the main reason for reliability effect. This study indicates that solar power contributes moderately in bulk system adequacy based on the system configuration.

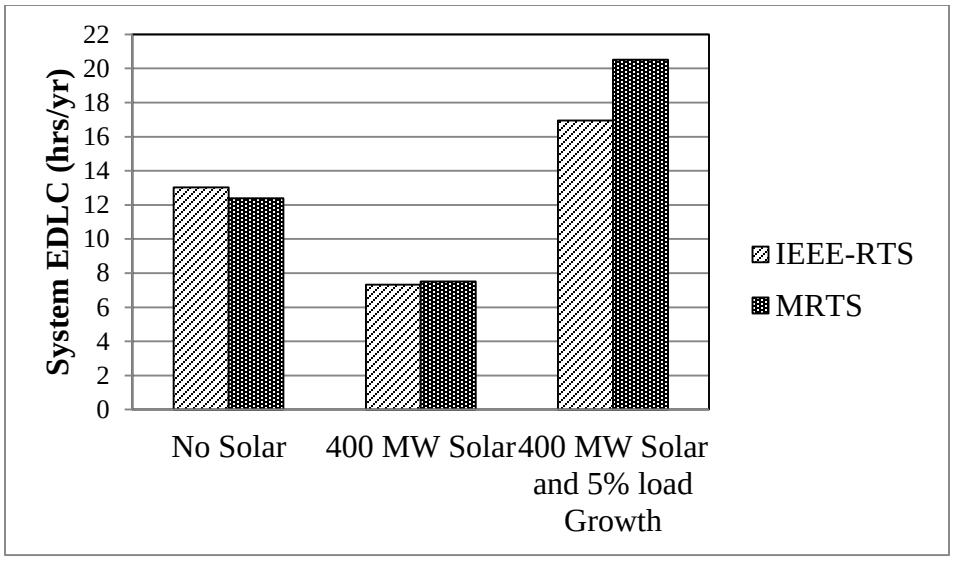

Figure 5.5: Impact of PV on the bulk system reliability of two different systems scenarios

5.4 Seasonal Solar Power Impact on Bulk System Adequacy

Solar irradiation is not constant throughout the year in a specific location. Solar irradiation varies considerably at different times in a year. The Swift Current solar radiation was utilized to study the seasonal solar power impact on bulk system adequacy. Four seasons were defined to conduct this study and the system peak load is different for each season in the IEEE-RTS. Table 5.1 shows the time period and the system peak loads for four different seasons in a year. It also shows that the system peak load is highest in winter followed by fall, summer and spring.

Table 5.1: Time periods for four different seasons and the associated IEEE-RTS system peak load

Season Name	Time Period	System Peak Load (MW)
Fall	September to November	2679
Winter	December to February	2850
Spring	March to May	2508
Summer	June to August	2565

Table 5.2 shows the five state PV capacity model developed for each season to assess the seasonal impact on bulk system adequacy. It can be seen that the probability of zero power output (or 100% capacity outage) is the highest in the winter season, and is equal to 0.8. The probability of rated output is zero in this season. Table 5.2 also shows the highest 100% capacity available probability for summer. The solar radiation values in the summer are higher than the other seasons at the Swift Current location.

Table 5.2: Capacity In Probability Table for the four seasons at the Swift Current location considering whole day radiation (including day and night)

Capacity In (%)	Probability (Fall)	Probability (Winter)	Probability (Spring)	Probability (Summer)
0	0.69052	0.80222	0.57713	0.48351
25	0.17326	0.15750	0.17283	0.16495
50	0.10142	0.03963	0.15127	0.15634
75	0.03223	0.00065	0.08025	0.13958
100	0.00256	0	0.01852	0.05562

A five state Capacity In Probability Table was also developed for each season considering only daytime solar radiation, and is shown in Table 5.3. The probability of obtaining 100% PV capacity is 0.08 for summer. This is the highest value among the four seasons. Table 5.3 shows a probability of 100% capacity outage for winter of 0.45960 which is the highest among four seasons. The reason is that the daytime radiation values in the winter are lower than those in the other seasons.

Table 5.3: Capacity In Probability Table for the four seasons at Swift Current location considering daytime radiation

Capacity In (%)	Probability (Fall)	Probability (Winter)	Probability (Spring)	Probability (Summer)
0	0.33722	0.45960	0.27254	0.20502
25	0.36584	0.44015	0.29591	0.25259
50	0.22874	0.10025	0.27063	0.24782
75	0.06284	0	0.13142	0.21017
100	0.00536	0	0.02949	0.08440

The IEEE-RTS was used to evaluate the seasonal impact of PV on bulk system adequacy. Figure 5.6 shows the variations in the EDLC for the four seasons with and without considering PV. The following steps were followed in the analysis.

1. The IEEE-RTS, without PV, was analyzed using MECORE for each season and the EDLC obtained for each season. Four load profiles based on the four seasons were utilized in the simulations.
2. A 400 MW solar farm using a whole day solar model from Table 5.2 was added to Bus 1 of the IEEE-RTS for each season in MECORE. During each season, a corresponding seasonal load profile was utilized in MECORE to obtain the EDLC. For instance, the EDLC for the winter season is obtained from MECORE using the winter PV model from Table 5.2 and the winter load profile. Similarly, other seasonal EDLC values were obtained using MECORE.

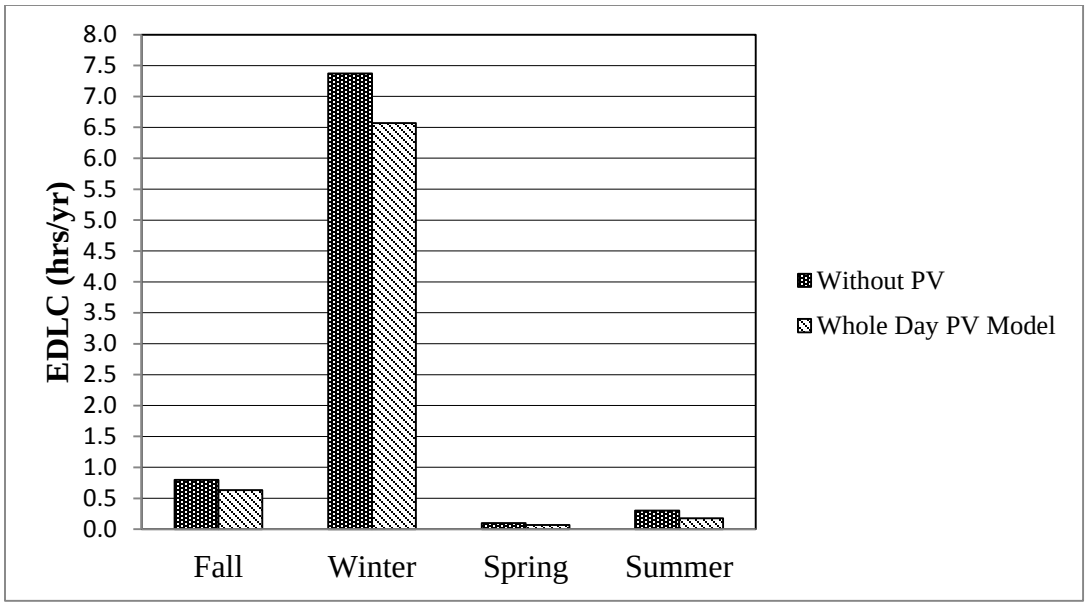

Figure 5.6: System EDLC of IEEE-RTS for the four seasons

Figure 5.6 shows that system EDLC without PV are 0.80 hrs/period, 7.37 hrs/period, 0.10 hrs/period and 0.30 hrs/period for fall, winter, spring and summer respectively. The system EDLC decreased from the without PV case EDLC during the fall season by approximately 21.25% due to the 400 MW whole day (including day and night) PV model injection. Similarly, the system EDLC values decreased from the without PV case by 11%, 32% and 41% for winter, spring and summer respectively when 400 MW whole day (including day and night) seasonal PV models were used in the MECORE simulations.

5.5 Solar Energy Reliability Benefit and Reliability Worth Analysis

Solar farm installations are continuously rising year by year due to environmental awareness. Solar energy reliability contributions to the system and customers' outage cost savings due to the solar energy provided, are important factors to consider. Two important factors such as solar penetration variations and solar seasonal contributions are examined in this chapter to

observe the solar energy reliability benefit to the system and associated customers' outage cost savings due to solar energy supplied.

5.5.1 Impact of Solar Penetration Variations on the Solar Energy Reliability Benefit and Reliability Worth

A study was done to assess the impact of solar penetration on energy reliability benefit and reliability worth. The Swift Current solar resource was utilized in this study. A 400 MW solar farm was assumed to be connected to Bus 1of IEEE-RTS. The solar capacity was then increased to 850 MW, 1460 MW and 2270 MW. The system peak load was held constant at 2850 MW in all cases. An annual solar model was used in the analysis. Table 5.4 shows the $EENS_S$ (Expected Energy Not Supplied with solar power present) and the EDC_S (Expected Damage Cost when solar power present) with for the different solar additions at Bus 1 of the IEEE-RTS. As the penetration increases, the system $EENS_S$ and EDC_S decreases. Table 5.4 also shows the $EENS_S$ and EDC_S tend to saturate at high solar injection levels.

Table 5.4: $EENS_S$ and EDC_S at various solar penetration levels in the IEEE-RTS

Penetration Level (MW)	$EENS_S$ (MWh/yr)	EDC_S (k$/yr)
400	1251.53	5281.46
850	1136.02	4794.01
1460	1098.13	4634.13
2270	1093.95	4616.49

The Expected Solar Reliability Benefit (ESRB) values were also calculated for the IEEE-RTS using Equation 4.1 for different penetration levels. The results are shown in Figure 5.7. The figure shows that the ESRB increases as the solar penetration is increased. The highest ESRB

saturates around 580 MWhr/yr for the 1460 MW and 2270 MW solar penetrations.

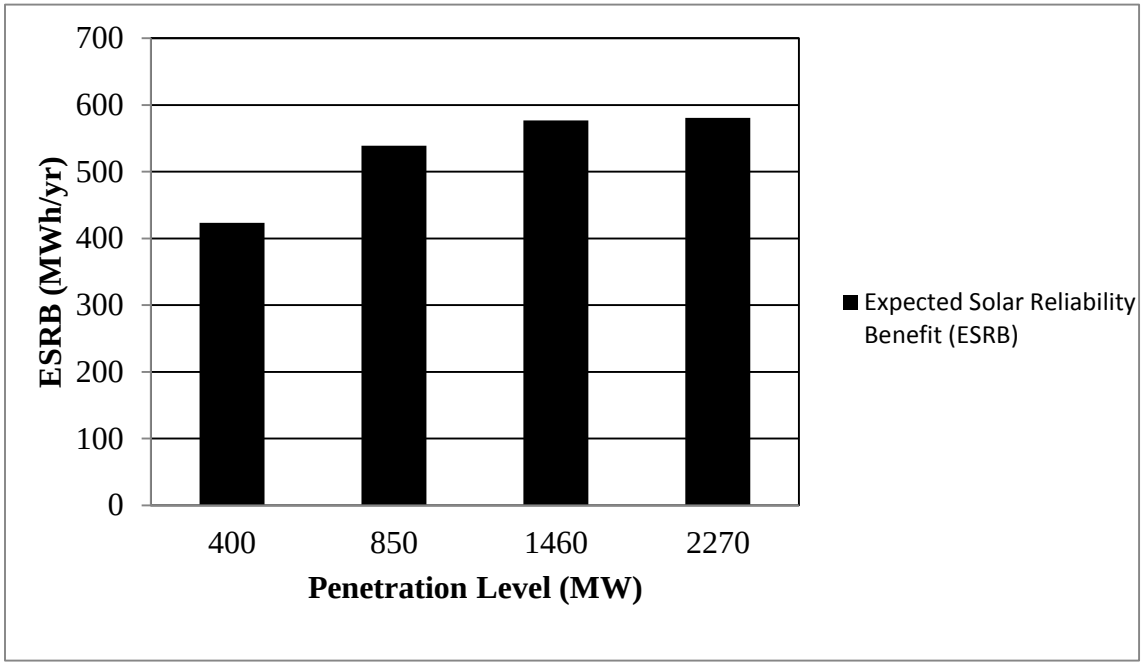

Figure 5.7: Solar reliability benefit for various penetration levels at 2850 MW peak load in the IEEE-RTS

The customers' outage cost savings due to solar energy supplied (CCS_S) were also calculated using Equation 4.2 for four different solar injection levels at Bus 1 of the IEEE-RTS. Figure 5.8 shows the values of CCS_S for the four different solar injection levels. The lowest cost saving was 1786.82 k$/yr for the 400 MW penetration. The CCS_S also tends to saturate around 2450 k$/yr for higher solar penetration levels.

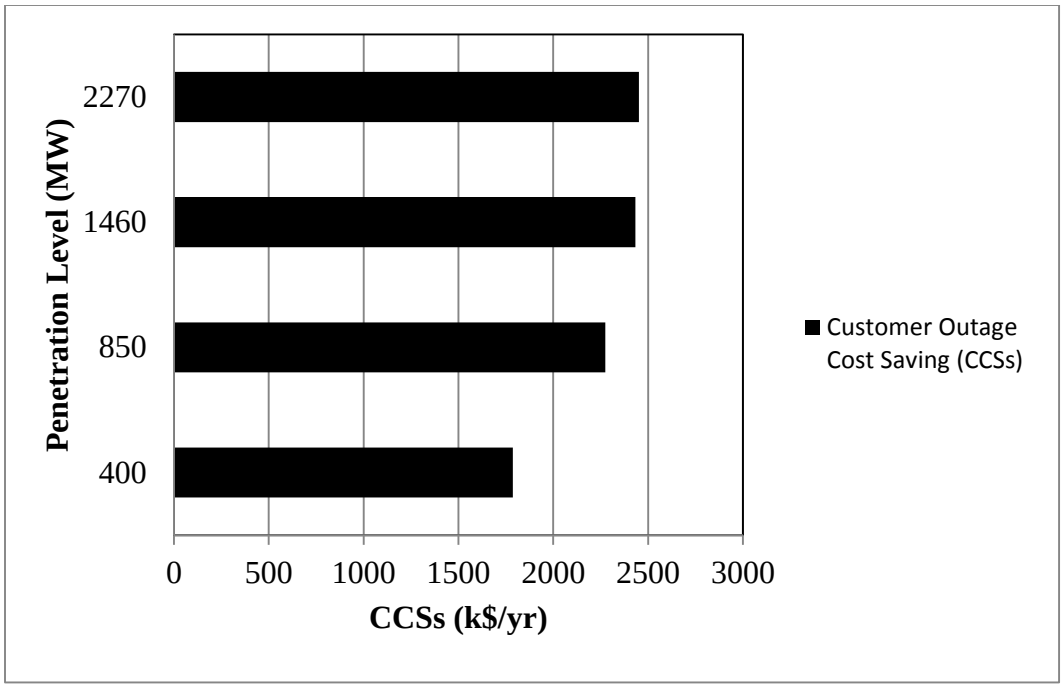

Figure 5.8: Customer outage cost saving (k$/yr) of various penetration levels at 2850 peak load at IEEE-RTS

5.5.2 Seasonality Impact on the Solar Energy Reliability Benefit and Reliability Worth

A study was investigated to assess the seasonality impact on the solar energy reliability benefit and reliability worth. Four cases were considered based on the four seasonal daytime solar models shown in Table 5.3 which were utilized to obtain $EENS_S$ and EDC_S using MECORE software. Table 5.5 shows the results of $EENS_S$ (Expected Energy Not Supplied when solar power is present) and EDC_S (Expected Damage Cost when solar power is present) for the 400 MW Solar farm at Bus 1 of the IEEE-RTS for different seasons.

Table 5.5: Seasonal $EENS_S$ and EDC_S for the 400 MW solar farm at Bus 1 of the IEEE-RTS

Season	**$EENS_S$ (MWh/period)**	**EDC_S (k$/period)**
Fall	46.73	197.20
Winter	681.67	2876.66
Spring	2.96	12.50
Summer	8.83	37.25

Equations 4.1 and 4.2 were used to calculate ESRB and CCS_S respectively for each season. $EENS_{NS}$ (Expected Energy Not Supplied when solar power is absent) and EDC_{NS} (Expected Damage Cost when solar power is absent) for each season were obtained using the MECORE software and corresponding seasonal load profiles. The values of $EENS_{NS}$ are 89.77 MWh/period, 994.47 MWh/period, 7.88 MWh/period and 28.96 MWh/period for fall, winter, spring and summer respectively. The values of EDC_{NS} for the fall, winter spring and summer are 378.83 k$/period, 4196.67 k$/period, 33.26 k$/period and 122.21 k$/period correspondingly. Table 5.6 shows the Expected Solar Reliability Benefit (ESRB) and the Customers' Cost Savings (CCS_S) for the four seasons. Reliability contribution for each season is also shown in Table 5.6 using the Equation 5.1.

$$\text{Reliability Contribution (\%)} = \frac{\text{ESRB of particular season}}{\text{EENS}_{\text{NS}} \text{ of corresponding season}} \times 100 \qquad (5.1)$$

Table 5.6: Seasonal contributions of ESRB and CCS_S

Season	ESRB **(MWh/period)**	**CCS_S (k$/period)**	**Reliability Contribution (%)**
Fall	43.04	181.63	47.94
Winter	312.8	1320.01	31.45
Spring	4.92	20.76	62.43
Summer	20.13	84.96	69.51

Table 5.6 shows that PV provides the highest reliability contribution of 69.51% in the summer and the lowest contribution of 31.45% in the winter. This is due to lower solar radiation values in winter at the Swift Current location.

5.6 Comparison between Solar and Wind in Bulk System

Wind and solar are two prominent sources of renewable energy in the present world. Utilities around the world are tending to replace conventional energy by wind or solar energy. Decision making on wind and/or solar farm establishment at a particular location requires comprehensive reliability and cost analysis of the system considering these renewable technologies. In this chapter, a comparison of reliability benefits is presented for a wind integrated bulk system and a solar integrated bulk system.

Wind integrated bulk system adequacy analysis is presented in Chapter 4. Solar integrated bulk system adequacy evaluation using solar radiation data from the Swift Current location is presented in previous sections of this chapter. Wind and solar reliability worth are also investigated in this study.

5.6.1 Adequacy Benefit Comparison between Wind and Solar

Bulk system adequacy benefits depends on the characteristics of the wind resource or solar resource connected to the system. Wind and solar radiation data from the Swift Current location are considered to assess the adequacy comparison between wind and solar. It is assumed that a 400 MW wind farm is connected to Bus 1 of the IEEE-RTS. The system EDLC obtained using the MECORE software is 8.80 hrs/yr. It was found that the system EDLC increased to 10.17 hrs/yr when the 400 MW wind capacity is replaced by PV capacity at the same bus. The reliability contribution of a 400 MW Swift Current wind farm is significantly higher than that of the solar farm with the Swift Current solar radiation data.

Further studies were conducted to assess the impact of increasing wind and solar power penetration on bulk system adequacy. The system EDLC values were obtained considering wind and solar capacities of 850 MW, 1460 MW and 2270 MW at Bus 1. System peak load was held constant at 2850 MW throughout the study. Figure 5.9 shows the results for both wind and solar.

Figure 5.9 shows that the system reliability increases with the increment in wind or solar power penetrations. Incremental reliability benefit decreases and reliability benefit tends to saturate at a certain high level of injections for both wind and solar. A close observation of Figure 5.9 indicates that a 400 MW Swift Current wind farm will provide a larger reliability benefit than an infinite amount of PV capacity connected at the same location. In this study wind gives better reliability than solar but it does not indicate that wind is always better than solar. This mainly depends on the resource strength at the geographical locations.

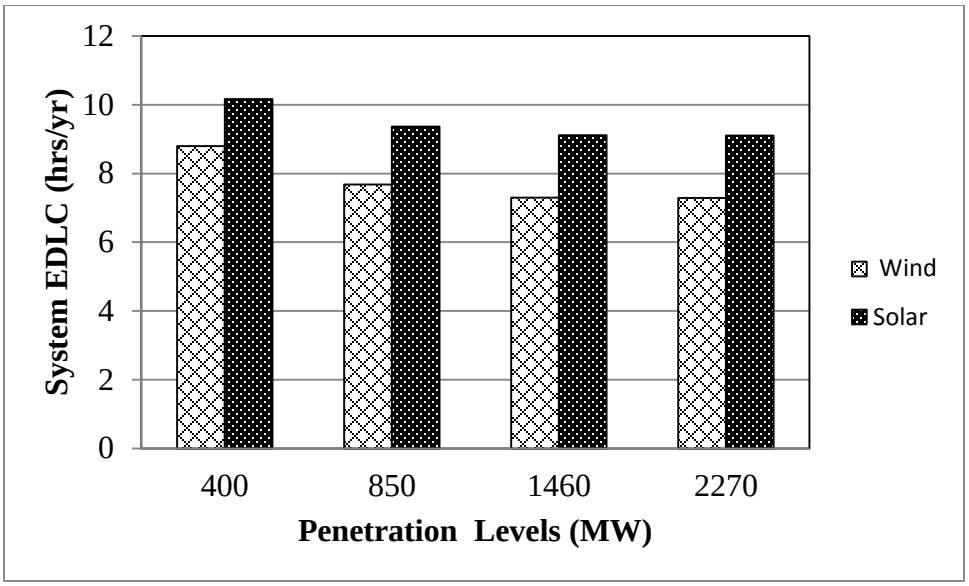

Figure 5.9: Adequacy benefit comparison between wind and solar in IEEE-RTS

5.6.2 Energy Reliability Benefit Comparison between Wind and Solar Energy Sources

Energy reliability benefit is compared between a wind integrated bulk system and a solar integrated bulk system. Swift Current wind resource and solar radiation data were used in the study of the IEEE-RTS. Two study cases were considered. A 400 MW wind farm was assumed to be connected at Bus 1 of the IEEE-RTS in the first case, and the $EENS_W$ and EDC_W were obtained using the MECORE software. The wind farm was replaced by a 400 MW solar park in the second case, and the $EENS_S$ and EDC_S were obtained. Table 5.7 shows the results for the two cases.

Table 5.7: Reliability indices for 400 MW wind integrated bulk system and 400 MW solar integrated bulk system

Resource Type	EENSw (MWh/yr)	EDCw (k$/yr)	EENSs (MWh/yr)	EDCs (k$/yr)
Wind	1102.12	4650.94	N/A	N/A
Solar	N/A	N/A	1291.53	5450.18

EWRB and ESRB were calculated for the IEEE-RTS using Equation 4.1 considering a 400 MW wind farm and a 400 MW solar farm connected to Bus 1 respectively. Results are shown in Figure 5.10 where wind is clearly superior to solar in regard to reliability benefit.

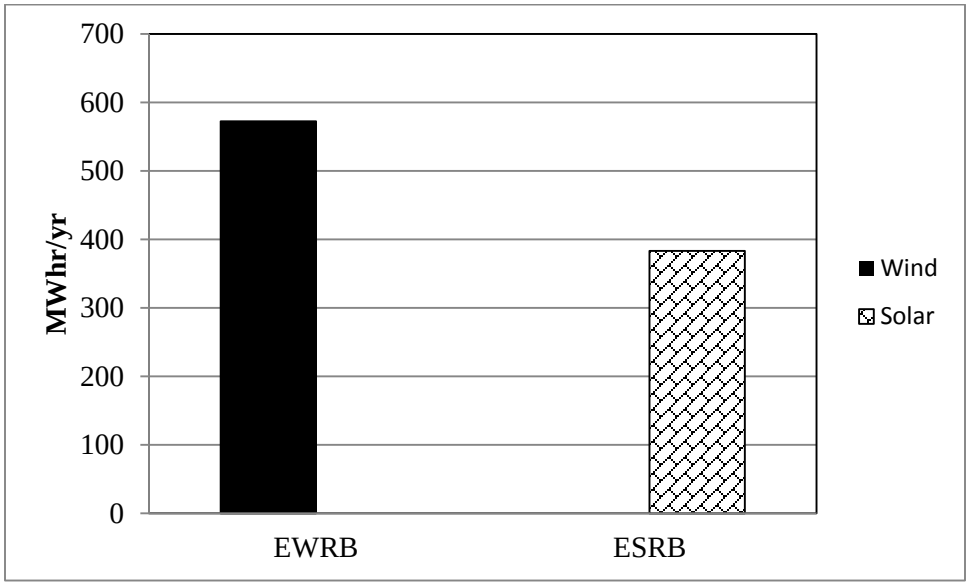

Figure 5.10: Expected reliability benefit with a 400 MW wind and a 400 MW solar farm connected individually at Bus 1 of the IEEE-RTS

The results show that the reliability benefit to the system by wind is higher than that by solar in this study. It is not always the case as the results depends on many factors such as the geographic location, network injection point etc. It is important that power system engineers carry

out comparative reliability studies as illustrated in this section in order to make proper decision on constructing wind or solar farms at specific locations.

5.7 Summary

The impact on the bulk system adequacy of increasing solar capacity in a power system was assessed at the beginning of this chapter. Solar power penetration was varied from 10.5% to 40% at Bus 1 of the IEEE-RTS in the study. The results show that the bulk system reliability improves with increasing penetration but the reliability benefit saturates at a certain high penetration level. It was found that the IPLCC due to PV addition at Bus 1 of the IEEE-RTS saturates at about 63 MW when 1460 MW or higher PV capacity is added to the system. At high penetration levels such as 1460 MW and above, the ESRB and CCS_S values were the highest and saturated.

Daytime solar reliability benefits were also investigated using the IEEE-RTS. The capacity available probability values for the daytime solar are higher than the whole day solar capacity available probability values, and the daytime solar model shows higher reliability benefits to the system than the whole day solar model. The reliability contribution of PV to bulk systems with different system configurations was also studied.

Seasonal impacts on bulk system adequacy were also investigated using PV capacity models developed for each season. Seasonal load profiles were developed to simulate the system in MECORE. Seasonal contribution to reliability worth and solar energy contribution were also assessed. It was found that the largest reliability improvement from PV addition was obtained during the summer season, and winter had the lowest reliability contribution among the four seasons due to lower values of solar radiation.

Adequacy benefit comparisons were studied for various solar and wind penetrations at Bus 1 of the IEEE-RTS considering the Swift Current data. A Wind integrated bulk system better reliability benefits for all penetration levels compared to a solar integrated bulk system. It was also shown that for the specific system data considered (Swift Current data in this case), the reliability benefit of infinite solar capacity in a solar integrated bulk system did not exceed the reliability benefit from a 400 MW wind farm. The wind integrated bulk system provided better system reliability benefits than those provided by the solar integrated bulk system.

6 SUMMARY AND CONCLUSIONS

Wind and solar energy are two important renewable energy sources for electric power generation in the present world. The rapid growth of these renewable energy sources is mainly due to growing public awareness to the environment. It has become a growing concern for power system planners and operators to integrate wind and/or solar power properly into the system and provide reliable power to the customers. This is why wind or solar integrated bulk power system adequacy analysis becomes important. The purpose of this research work was to evaluate the contributions of wind or solar energy sources to the reliability of the overall bulk system depending on many factors and assess their contribution to the bulk system adequacy.

Chapter 1 introduces the basic concepts of power system reliability. This chapter also includes a description of a power system with wind and solar energy. The problem statement and the research objectives are presented in this chapter.

Chapter 2 describes detail explanations of the techniques for bulk system adequacy assessment and the reliability indices used to measure bulk system reliability. Monte Carlo Simulation was introduced in this chapter with discussion on the non-sequential methods. The Non-sequential state sampling method used in the MECORE software was briefly described. This chapter also describes the features and limitations of the MECORE software that was used to obtain the reliability indices in the studies presented in the thesis. The composite test system IEEE-RTS was introduced in this chapter with relevant generation, load, and transmission data. This system is used and modified to carry out selected studies on bulk systems integrated with wind and solar power.

Chapter 3 presents the developments of wind and solar models for bulk system adequacy assessment. Swift Current and Saskatoon hourly wind speed data obtained from Environment

Canada are utilized to develop models. Five state wind power models for both Swift Current and Saskatoon were developed using an apportioning technique to conduct analysis using MECORE software. The developed PV model is also explained in this chapter. Swift Current solar radiation data were obtained from the SIPSREL+ software. The BP 4175T PV array was used in analytical technique to convert the hourly solar radiation data to hourly solar power data. Five- state daytime and whole-day PV power models were developed and used in bulk system reliability studies in Chapters 4 and 5.

Chapter 4 describes the wind integrated bulk system considering various factors such as the strength of the wind resource, the point of wind integration in the power grid, the generation system configuration etc. The key factors affecting bulk system adequacy are highlighted in this chapter. At the same time, how these factors influence the reliability worth and reliability benefit of the bulk system are also explained. The impact of transmission line outages on the reliability indices is shown at the beginning of this chapter. In a study to assess the impact of wind resource strength on bulk system reliability, it was found that the Swift Current wind resource shows better reliability benefits than the Saskatoon wind resource. This was due to higher hourly wind speed at the Swift Current site than that of Saskatoon. The reliability contribution of wind resources on power systems with different configurations was investigated using comparative studies on the MRTS and the IEEE-RTS. The IEEE-RTS has a strong transmission system and a relatively weak generation system. The MRTS was developed to create a system with weak transmission and a relatively strong generation system. The MRTS showed less reliability benefit than the IEEE-RTS while 5% load growth in addition with a 400 MW wind power introduced in each systems. The MRTS transmission system is highly stressed compared to the IEEE-RTS transmission system. This caused the MRTS to be less reliable when the load is increased.

Impact of wind injection point in the grid network is also studied in this chapter. Wind connected to a strong bus based on network topology provides better reliability benefit than wind connected to a relatively weak bus. Studies done to investigate the impact of wind power diversification show that totally independent wind farms provide better reliability benefit than other cases where wind farms are highly correlated. These wind farms, however need to be connected at grid points with good network configuration to get optimum reliability benefits. Independent wind farms provide better reliability benefits and outage cost savings in a system compared to dependent wind farms and moderately dependent wind farms. Energy reliability benefits and customers' outage cost savings due to the Swift Current wind generation was lower when connected to a weak network bus.

Chapter 5 presents an adequacy analysis of the solar integrated bulk system considering various factors. Swift Current solar radiation data were used to analyse solar integrated bulk system adequacy. Reliability contributions and outage cost savings due to solar power in the bulk system were also investigated considering different penetration levels and seasonal variations of solar radiation. A brief comparison between wind integrated bulk and solar integrated bulk systems was done to consider the best option for renewable energy planning.

Adequacy analysis was conducted to assess the impact of PV penetration in power systems. Reliability benefits were lower at low penetration levels but at higher penetration levels, the reliability benefits became saturated. The IPLCC decreases with incremental addition of PV capacity, and at a certain high penetration level there is no further increase in the IPLCC. The benefit in solar energy contributions and customers' outage cost savings tend to saturate at a high penetration level. The use of daytime solar models provides a higher reliability contribution than the whole day solar models as sunlight is absent at night. The reliability contribution of PV

resources on power systems with different configurations was investigated using comparative studies on the MRTS and the IEEE-RTS. The MRTS showed less reliability benefit than that of the IEEE-RTS when a 400 MW PV park was added. The reliability contribution of PV in the summer season is significantly higher than that in other seasons due to the high solar radiation values in the summer. Seasonal impact on reliability worth and reliability benefit was also examined where summer provides best reliability benefit and worth than other seasons.

Comparisons are also done between solar and wind using wind and solar irradiation data from the Swift Current location. The reliability benefits from the wind resource were better than that from solar. The renewable energy benefits from wind resource is also significantly better than that of the solar. This is not a general conclusion as reliability benefits for wind and solar depend on the geographic location. The factors examined in this chapter are essential to understand solar power behaviour on the bulk system. Solar energy reliability benefits and customers' outage cost savings for the system can be very different based on these factors.

This thesis presents some fundamental concepts and important factors that need to be considered in wind or solar integration to the bulk system. The methodologies developed to incorporate five state wind and solar models in the MECORE software to obtain bulk system reliability indices are presented and illustrated with examples and case studies. The results and explanations provided in this thesis can assist power system engineers to make reliable and economic plans for wind or solar energy integration to the bulk system.

REFERENCES

1. R. Billinton and R.N. Allan, “Reliability Evaluation of Power Systems”, Second Edition, Plenum Press, New York, 1996.
2. R. Billinton and R. N. Allan, Reliability Evaluation of Engineering Systems: Concepts and Techniques. Springer, 1992.
3. “Power System Reliability in Perspective,” IEE J. Electronics Power, vol. 30, pp. 231 – 236, 1984.
4. R. Billinton, “Criteria Used by Canadian Utilities in the Planning and Operation of Generating Capacity,” IEEE Transactions on Power Systems, vol. 3, no. 4, pp. 1488 – 1493, 1988.
5. “Wind Installed Capacity around Canada -2014”- http://canwea.ca/wind-energy/installed-capacity/
6. "GWEC, Global Wind Report Annual Market Update", http://www.gwec.net/?id=180
7. “Solar Power”-http://en.wikipedia.org/wiki/Solar_power
8. “National survey report of PV power applications in Canada 2013’’- http://www.cansia.ca/market-intelligence/solar-photovoltaics
9. ‘REN 21-Renewables 2014 Global Status Report’- http://www.ren21.net/status-of-renewables/global-status-report/
10. R. Billinton, M. Fotuhi-Firuzabad and L. Bertling, “Bibliography on the application of probability methods in power system reliability evaluation1996-1999,” Power Syst. IEEE Trans., vol. 16, no. 4, pp. 595-602, 2001.

11. R. N. Allan, R. Billinton, A. M. Breipohl and C. H. Grigg, "Bibliography on the application of probability methods in power system reliability evaluation: 1987-1991,"Power Systems, IEEE Transactions on, vol. 9, pp. 41-49, 1994.

12. R. Billinton, "Bibliography on the on the application of probability methods in power system reliability evaluation;" Power Appar., Syst. IEEE Transactions, vol. PAS-91, no.2, pp. 649-660, 1972.

13. R. Billinton and D. Huang, "Basic considerations in generating capacity adequacy evaluation," in Electrical and Computer Engineering, 2005. Canadian Conference on, 2005, pp. 611-614.

14. R. Billinton and R.N. Allan, "Generating capacity- basic probability methods," - in Reliability evaluation of power systems, 2nd ed., New York: Plenum Press, 1996, pp.18-82.

15. Y. Li, "Bulk system reliability evaluation in a deregulated power industry," University of Saskatchewan, Saskatoon, 2003.

16. W. Wangdee and R. Billinton, "Considering load-carrying capability and wind speed correlation of WECS in generation adequacy assessment," Energy conversion, IEEE Trans., vol. 21, no. 3, pp. 734-741, 2006.

17. R. Billinton and G. Bai, "Generating capacity adequacy associated with wind energy," IEEE Trans. Energy Convers., vol. 19, no. 3, pp. 641-646, 2004.

18. R. Karki and P. Hu, "Wind power simulation model for reliability evaluation," in Electrical and Computer Engineering, 2005. Canadian Conference on, 2005, pp. 541–544.

19. Y. Gao, "Adequacy assessment of electric power systems incorporating wind and solar energy," MSc thesis, University of Saskatchewan, 2006.

20. M. R. Haghifam and M. Omidvar, “Wind Farm Modeling in Reliability Assessment of Power System,” in 9th International Conference on Probabilistic Methods Applied to Power Systems, 2006, pp. 1–5.

21. R. Karki, P. Hu, and R. Billinton, “A Simplified Wind Power Generation Model for Reliability Evaluation,” IEEE Trans. Energy Convers., vol. 21, no. 2, pp. 533–540, Jun. 2006.

22. M. S. Miranda and R. W. Dunn, “Spatially correlated wind speed modelling for generation adequacy studies in the UK,” in Power Engineering Society General Meeting, 2007. IEEE, 2007, pp. 1–6.

23. F. Vallée, J. Lobry, and O. Deblecker, “Impact of the Wind Geographical Correlation Level for Reliability Studies,” IEEE Trans. power Syst., vol. 22, no. 4, pp. 2232–2239, 2007.

24. M. Milligan and K. Porter, “Wind capacity credit in the United States,” *2008* IEEE Power Energy Soc. Gen. Meet. - Convers. Deliv. Electr. Energy 21st Century, pp. 1–5, Jul. 2008.

25. J. Hetzer, D. C. Yu, and K. Bhattarai, “An Economic Dispatch Model Incorporating Wind Power,” IEEE Trans. Energy Convers., vol. 23, no. 2, pp. 603–611, 2008.

26. A. Coelho and R. Castro, "Modeling and validation of PV power output with solar tracking," in Power Engineering, Energy and Electrical Drives (POWERENG), 2011International Conference on, 2011, pp. 1-6.

27. C. P. Cameron, W. E. Boyson and D. M. Riley, "Comparison of PV system performance-model predictions with measured PV system performance," in Photovoltaic Specialists Conference, 2008. PVSC'08. 33rd IEEE, 2008, pp. 1-6.

28. N. Kishor, S. R. Mohanty, M. Villalva and E. Ruppert, "Simulation of PV array output power for modified PV cell model," in Power and Energy (PECon), 2010 IEEE International Conference on, 2010, pp. 533-538.

29. R. Billinton and W. Li, Reliability Assessment of Electric Power Systems using MonteCarlo Methods. Springer, 1994.

30. R. Billinton and R. N. Allan, Reliability Evaluation of Power Systems. Springer, 1996.

31. R. Billinton and R. Karki, "Maintaining supply reliability of small isolated power systems using renewable energy," in Generation, Transmission and Distribution, IEEE Proceedings-, 2001, pp. 530-534.

32. R. Billinton and R. Karki, "Reliability/cost implications of utilizing photovoltaics in small isolated power systems," Reliab. Eng. Syst. Saf., vol. 79, pp. 11-16, 2003.

33. T. Skakum, "Reliability of a Generating System Containing Photovoltaic Power Generation," M.Sc thesis, University of Saskatchewan, Canada, 1997.

34. Ahmad Alferidi, "Evaluating the reliability contribution of photovoltaics in electric power systems"- M.Sc. thesis, University of Saskatchewan, Canada, 2012.

35. C. Singh and A. Lago-Gonzalez, "Reliability Modeling of Generation System Including Unconventional Energy Sources", IEEE Transaction on Power Apparatus and System, Vol. PAS-104, No.5, 1985, pp. 1049-1056.

36. Yi Gao, "Adequacy assessment of composite generation and transmission systems incorporating wind energy conversion systems"-Ph.D. thesis, University of Saskatchewan, Canada, 2010

37. R. Billinton, "Elements of Composite System Reliability Evaluation", Canadian Electrical Association System Planning and Operation Section, Spring Meeting, 1976.

38. W. Li, “Installation Guide and User's Manual for the MECORE Program", July, 1998.

39. R. Billinton, and A. Sankarakrishnan, “A Comparison of Monte Carlo Simulation Techniques for Composite Power System Reliability Assessment”, Proceedings of the IEEE Wescanex 95 Conference, May 1995, pp. 145-150.

40. Nahun Bulmaro Vega Hernandez, “Load forecast uncertainty considerations in Bulk Electrical System Adequacy Assessment’’- M.Sc. thesis, University of Saskatchewan, Canada, 2009.

41. E. J. Henley and H. Kumamoto, Probability Risk Assessment: Reliability Engineering, Design and Analysis, IEEE Press, New York, 1992.

42. R. Billinton and W. Li, “Hybrid Approach for Reliability Evaluation of Composite Generation and Transmission Systems Using Monte Carlo Simulation and Enumeration Technique,” IEE Proceedings-C, Vol. 138, No. 3, 1991, pp. 233-241.

43. M.V.F. Pereira, M.E.P. Maceira, G.C. Olivera and L.M.V.G. Pinto, “Combining analytical models and Monte Carlo Techniques in probabilistic power system analysis”, IEEE Transactions on power systems, Vol. 7, No. 1, February 1992, pp. 265-272.

44. R. Billinton. And W. Li, "A System State Transition Sampling Method for Composite System Reliability Evaluation", IEEE Transactions on Power Systems, Vol. 8, No. 3, Aug. 1993, pp. 761-771.

45. R. Billinton, S. Kumar, N. Chowdhury, K.Chu, K. Debnath, L. Goel, E. Khan, P. Kos, G. Nourbakhsh, J. Oteng-Adjei, “A Reliability Test System for Educational Purposes–Basic Data”, IEEE Transactions on Power Systems, Vol. 4, No. 3, August 1989, pp. 1238-1244.

46. R. Billinton and W.Wangdee, “Impact of Utilizing Sequential and Non-Sequential Simulation Techniques in Bulk Electric System Reliability Assessment”, IEE Generation, Transmission and Distribution, Vol.152, No. 5, September 2005, pp.623-628.

47. IEEE Task Force, “IEEE Reliability Test System,” IEEE Transactions on Power Apparatus and Systems, Vol. PAS-98, Nov/Dec. 1979, pp. 2047-2054.

48. Environment Canada, “Wind Speed,” ec.gc.ca. [online] Available: https://ec.gc.ca/default.asp?lang=en&n=FD9B0E51-1 [Accessed: Feb. 25, 2015]

49. P. Giorsetto and K.F. Utsurogi, “Development of A New Procedure for Reliability Modeling of Wind Turbine Generators”, IEEE Transactions on Power Apparatus and Systems, Vol. PAS-102, No. 1, 1983, pp.134-143.

50. R. Billinton and C. Wee, Derated State Modelling of Generating Units, Report prepared for Saskatchewan Power Corporation, September 1985.

51. Xiaoming Cao, Adequacy Assessment of a Combined Generating System Containing Wind Energy Conversion System, M.Sc. thesis, University of Saskatchewan, 1994.

52. John A. Duffie and William A. Beckman, Solar Engineering of Thermal Process. New York: John Wiley and Sons Inc., 1980.

53. “Reliability and cost evaluation of small isolated power systems containing photovoltaic and wind energy’’- A Ph.D. thesis by Rajesh Karki, University of Saskatchewan, 2000.

54. BP Solar BP4175T, "175W Photovoltaic Module," Available: http://www.amerescosolar.com/sites/default/files/bp4175t.pdf

55. Jaeseok Choi, Jeongje Park, M. Shahidehpour and R. Billinton, "Assessment of CO2 reduction by renewable energy generators," in Innovative Smart Grid Technologies (ISGT), 2010, 2010, pp. 1-5.

56. Dinesh Dhungana, “Incorporating correlation in the adequacy evaluation of wind integrated power systems”- M.Sc. thesis, University of Saskatchewan, Canada, 2013.

APPENDIX

Basic data for the IEEE-RTS are shown in Table A 1- A 7

Table A 1: Bus data for the IEEE-RTS

Bus No.	Load (p.u.)		P_g	Q_{max}	Q_{min}	V_0	V_{max}	V_{min}
	Active	Reactive						
1	1.08	0.22	1.92	1.20	-0.75	1.00	1.05	0.95
2	0.97	0.20	1.92	1.20	-0.75	1.00	1.05	0.95
3	1.80	0.37	0.00	0.00	0.00	1.00	1.05	0.95
4	0.74	0.15	0.00	0.00	0.00	1.00	1.05	0.95
5	0.71	0.14	0.00	0.00	0.00	1.00	1.05	0.95
6	1.36	0.28	0.00	0.00	0.00	1.00	1.05	0.95
7	1.25	0.25	3.00	2.70	0.00	1.00	1.05	0.95
8	1.71	0.35	0.00	0.00	0.00	1.00	1.05	0.95
9	1.75	0.36	0.00	0.00	0.00	1.00	1.05	0.95
10	1.95	0.40	0.00	0.00	0.00	1.00	1.05	0.95
11	0.00	0.00	0.00	0.00	0.00	1.00	1.05	0.95
12	0.00	0.00	0.00	0.00	0.00	1.00	1.05	0.95
13	2.65	0.54	5.91	3.60	0.00	1.00	1.05	0.95
14	1.94	0.39	0.00	3.00	-0.75	1.00	1.05	0.95
15	3.17	0.64	2.15	1.65	-0.75	1.00	1.05	0.95
16	1.00	0.20	1.55	1.20	-0.75	1.00	1.05	0.95
17	0.00	0.00	0.00	0.00	0.00	1.00	1.05	0.95
18	3.33	0.68	4.00	3.00	-0.75	1.00	1.05	0.95
19	1.81	0.37	0.00	0.00	0.00	1.00	1.05	0.95
20	1.28	0.26	0.00	0.00	0.00	1.00	1.05	0.95
21	0.00	0.00	4.00	3.00	-0.75	1.00	1.05	0.95
22	0.00	0.00	3.00	1.45	-0.90	1.00	1.05	0.95
23	0.00	0.00	6.60	4.50	-0.75	1.00	1.05	0.95
24	0.00	0.00	0.00	0.00	0.00	1.00	1.05	0.95

Table A 2: Line data for the IEEE-RTS

Line No.	Bus		R	X	B/2	Tap	Current Rating (p.u.)	Failure Rate (Occ./yr)	Repair Time (hrs.)
	I	J							
1	1	2	0.026	0.0139	0.2306	1	1.75	0.24	16
2	1	3	0.0546	0.2112	0.0286	1	1.75	0.51	10
3	1	5	0.0218	0.0845	0.0115	1	1.75	0.33	10
4	2	4	0.0328	0.1267	0.0172	1	1.75	0.39	10
5	2	6	0.0497	0.192	0.026	1	1.75	0.48	10
6	3	9	0.0308	0.119	0.0161	1	1.75	0.38	10
7	3	24	0.0023	0.0839	0	1	4	0.02	768
8	4	9	0.0268	0.1037	0.0141	1	1.75	0.36	10
9	5	10	0.0228	0.0883	0.012	1	1..75	0.34	10
10	6	10	0.0139	0.0605	1.2295	1	1.75	0.33	35
11	7	8	0.0159	0.0614	0.0166	1	1.75	0.3	10
12	8	9	0.0427	0.1651	0.0224	1	1.75	0.44	10
13	8	10	0.0427	0.1651	0.0224	1	1.75	0.44	10
14	9	11	0.0023	0.0839	0	1	4	0.02	768
15	9	12	0.0023	0.0839	0	1	4	0.02	768
16	10	11	0.0023	0.0839	0	1	4	0.02	768
17	10	12	0.0023	0.0839	0	1	4	0.02	768
18	11	13	0.0061	0.0476	0.05	1	5	0.4	11
19	11	14	0.0054	0.0418	0.044	1	5	0.39	11
20	12	13	0.0061	0.0476	0.05	1	5	0.4	11
21	12	23	0.0124	0.0966	0.1015	1	5	0.52	11
22	13	23	0.0111	0.0865	0.0909	1	5	0.49	11
23	14	16	0.005	0.0389	0.0409	1	5	0.38	11
24	15	16	0.0022	0.0173	0.0364	1	5	0.33	11
25	15	21	0.0063	0.049	0.0515	1	5	0.41	11
26	15	21	0.0063	0.049	0.0515	1	5	0.41	11
27	15	24	0.0067	0.0519	0.0546	1	5	0.41	11
28	16	17	0.0033	0.0259	0.0273	1	5	0.35	11
29	16	19	0.003	0.0231	0.0243	1	5	0.34	11
30	17	18	0.0018	0.0144	0.0152	1	5	0.32	11
31	17	22	0.0135	0.1053	0.1106	1	5	0.54	11
32	18	21	0.0033	0.0259	0.0273	1	5	0.35	11
33	18	21	0.0033	0.0259	0.0273	1	5	0.35	11
34	19	20	0.0051	0.0396	0.0417	1	5	0.38	11
35	19	20	0.0051	0.0396	0.0417	1	5	0.38	11
36	20	23	0.0028	0.0216	0.0228	1	5	0.34	11
37	20	23	0.0028	0.0216	0.0228	1	5	0.34	11
38	21	22	0.0087	0.0678	0.0712	1	5	0.45	11

Table A 3: Generator data for the IEEE-RTS

Unit No.	Bus No.	Rating (MW)	Failure Rate (Occ./yr)	Repair Time (hrs)	Failure Prob.
1	22	50	4.42	20	0.01
2	22	50	4.42	20	0.01
3	22	50	4.42	20	0.01
4	22	50	4.42	20	0.01
5	22	50	4.42	20	0.01
6	22	50	4.42	20	0.01
7	15	12	2.98	60	0.02
8	15	12	2.98	60	0.02
9	15	12	2.98	60	0.02
10	15	12	2.98	60	0.02
11	15	12	2.98	60	0.02
12	15	155	9.13	40	0.04
13	7	100	7.3	50	0.04
14	7	100	7.3	50	0.04
15	7	100	7.3	50	0.04
16	13	197	9.22	50	0.05
17	13	197	9.22	50	0.05
18	13	197	9.22	50	0.05
19	1	20	19.47	50	0.1
20	1	20	19.47	50	0.1
21	1	76	4.47	40	0.02
22	1	76	4.47	40	0.02
23	2	20	9.13	50	0.1
24	2	20	9.13	50	0.1
25	2	76	4.47	40	0.02
26	2	76	4.47	40	0.02
27	23	155	9.13	40	0.04
28	23	155	9.13	40	0.04
29	23	350	7.62	100	0.08
30	18	400	7.96	150	0.12
31	21	400	7.96	150	0.12
32	16	155	9.13	40	0.04

Table A 4: The weekly peak load as percent of annual peak

Week	Peak Load	Week	Peak Load	Week	Peak Load	Week	Peak Load
1	86.2	14	75	27	75.5	40	72.4
2	90	15	72.1	28	81.6	41	74.3
3	87.8	16	80	29	80.1	42	74.4
4	83.4	17	75.4	30	88	43	80
5	88	18	83.7	31	72.2	44	88.1
6	84.1	19	87	32	77.6	45	88.5
7	83.2	20	88	33	80	46	90.9
8	80.6	21	85.6	34	72.9	47	94
9	74	22	81.1	35	72.6	48	89
10	73.7	23	90	36	70.5	49	94.2
11	71.5	24	88.7	37	78	50	97
12	72.7	25	89.6	38	69.5	51	100
13	70.4	26	86.1	39	72.4	52	95.2

Table A 5: Daily peak load as percentage of weekly load

Day	Peak Load
Monday	93
Tuesday	100
Wednesday	98
Thursday	96
Friday	94
Saturday	77
Sunday	75

Table A 6: Hourly peak load as percentage of daily peak

Hour	Winter Weeks 1-8&44-52		Summer Weeks 18-30		Spring/Fall Weeks 9-17 & 31-43	
	Weekday	Weekend	Weekday	Weekend	Weekday	Weekend
12-1am	67	78	64	74	63	75
1-2	63	72	60	70	62	73
2-3	60	68	58	66	60	69
3-4	59	66	56	65	58	66
4-5	59	64	56	64	59	65
5-6	60	65	58	62	65	65
6-7	74	66	64	62	72	68
7-8	86	70	76	66	85	74
8-9	95	80	87	81	95	83
9-10	96	88	95	86	99	89
10-11	96	90	99	91	100	92
11-noon	95	91	100	93	99	94
Noon-1pm	95	90	99	93	93	91
1-2	95	88	100	92	92	90
2-3	93	87	100	91	90	90
3-4	94	87	97	91	88	86
4-5	99	91	96	92	90	85
5-6	100	100	96	94	92	88
6-7	100	99	93	95	96	92
7-8	96	97	92	95	98	100
8-9	91	94	92	100	96	97
9-10	83	92	93	93	90	95
10-11	73	87	87	88	80	90
11-12	63	81	72	80	70	85

Table A 7: The RTS 20-step load duration curve data

Load Level	Probability
1.00	0.00023
0.99	0.00011
0.98	0.00057
0.97	0.00171
0.95	0.00171
0.93	0.00331
0.92	0.00616
0.90	0.0097
0.88	0.01153
0.86	0.0161
0.85	0.02363
0.83	0.02546
0.81	0.02386
0.80	0.03311
0.78	0.03459
0.76	0.01632
0.75	0.08219
0.70	0.23162
0.60	0.21553
0.50	0.26256

Table A 8: The electrical characteristics of BP 4175T

Description	**Value**
Maximum power	175 Watt
Voltage at maximum power	35.4 Volt
Current at maximum power	4.94 Ampere
Short circuit current	5.45 Ampere
Open Circuit voltage	43.6 Volt
Module efficiency	14.0 %
Tolerance	-3/+5%
Nominal voltage	24 Volt
Limiting reverse current	5.45 Ampere
Maximum series fuse rating	20 Ampere
Application class (according to IEC 61730-2007)	Class A
Maximum system voltage	1000 Volt (IEC 61730-2007)